Precambrian Research 320 (2019) 350–370

Contents lists available at ScienceDirect

Precambrian Research

journal homepage: www.elsevier.com/locate/precamres

A new Siberian record of the ~1.0 Gyr-old Maya superchron

Vladimir E. Pavlov[a,b,*], Yves Gallet[c], Peter Yu. Petrov[d]

[a] Institute of Physics of the Earth, Russian Academy of Science, Moscow, Russia
[b] Kazan Federal University, Kazan, Russia
[c] Institut de Physique du Globe de Paris, Sorbonne Paris Cité, Université Paris Diderot, CNRS, F-75005 Paris, France
[d] Geological Institute, Russian Academy of Science, Moscow, Russia

ARTICLE INFO

Keywords:
Precambrian
Siberia
Magnetostratigraphy
Superchron
Apparent polar wander path

ABSTRACT

We report new magnetostratigraphic data from the Late Mesoproterozoic Linok Formation consisting of clayed carbonates, together with paleomagnetic data from the Neoproterozoic carbonate Sukhaya Tunguska, Burovaya and Turukhansk formations, located in the Turukhansk region (northwestern Siberian platform). We also re-analyzed demagnetization data previously obtained from the Derevnya Formation. Paleomagnetic analyses revealed up to four magnetization components. First, a steep-inclination component, likely of recent origin, is isolated in all sections in the low temperature range. Second, a magnetization is recovered in most samples between ~250 °C and ~350–400 °C. It shows a single magnetic polarity and is interpreted as a remagnetization acquired during the Kiaman Permo-Carboniferous reverse superchron. Third, a magnetization component is isolated between ~400 °C and ~500 °C in samples from the Burovaya and Turukhansk formations. This component is interpreted as a remagnetization that occurred before the end of the Neoproterozoic. A fourth high-temperature (HT) magnetization component is observed up to ~575 °C in samples from the Linok and Burovaya formations and up to ~680 °C for those of the Derevnya and Turukhansk formations. A series of magnetic polarity reversals is observed in the lower and middle parts of the Linok Formation, whereas a single polarity interval is found in its upper part. The syn-depositional origin of this magnetization is attested by positive reversal, conglomerate and fold tests. The HT magnetization component isolated in the Derevnya and Burovaya formations shows a single magnetic polarity. Its primary origin is supported by the fact that the Derevnya and Burovaya HT mean directions are positioned in the continuity of the directional evolution observed through the Linok Formation. It is further constrained by very consistent Late Mesoproterozoic to Early Neoproterozoic apparent polar wander paths obtained from different regions of the Siberian platform. A single magnetic polarity reversal is observed in a ~40 m-thick section of the Turukhansk Formation. The HT directions found in the upper part of the Linok Formations, over a stratigraphic thickness of ~200 m, and in the Derevnya and Burovaya formations strengthen the existence of the normal polarity Maya superchron around 1.0 Ga, at the transition between the Mesoproterozoic and the Neoproterozoic.

1. Introduction

Tracing the long-term geomagnetic field evolution during the Precambrian is necessary for understanding the operational modes of our planet, especially the interactions between the different Earth's envelopes, but also for providing age constraints on the growth of the inner core (e.g. Aubert et al., 2009; Gallet et al., 2012; Olson et al., 2013; Biggin et al., 2015; Landeau et al., 2017). In the latter case, the objective is to identify a possible evolution in the geodynamo regime before and after the inner core nucleation, the age of this transition yielding a constraint on the long-term cooling of the Earth (e.g. Labrosse, 2003; Aubert et al., 2009). Recent data on core thermal conductivity indicates the point of transition is as recent as the Early Paleozoic (around 500 Ma; Pozzo et al., 2012), or not beyond the Neoproterozoic (< 1 billion years; e.g. Olson et al., 2013). There are others who argue in favor of lower thermal conductivity values, and therefore for a much older, perhaps several billion years-old inner core nucleation (e.g. Konôpková et al., 2016). Paleointensity determinations, which are currently too scarce for characterizing a robust long-term evolution in the geomagnetic field behavior (Biggin et al, 2015; Smirnov et al., 2016), may not be a suitable parameter to constrain the issue (Landeau et al., 2017). Gallet et al. (2012) and Smirnov et al. (2016) suggest instead an investigation into the evolution in Precambrian geomagnetic reversal frequency.

* Corresponding author.
E-mail address: pavlov.ifz@gmail.com (V.E. Pavlov).

https://doi.org/10.1016/j.precamres.2018.11.005
Received 13 April 2018; Received in revised form 22 September 2018; Accepted 11 November 2018
Available online 16 November 2018
0301-9268/

A limited paleomagnetic database has hitherto supported the suggestion that geomagnetic field reversals were less frequent during the Precambrian than during the Phanerozoic (e.g. Roberts and Piper, 1989; Dunlop and Yu, 2004). More recently, however, several magnetostratigraphic datasets showed the occurrence of numerous polarity reversals during different Precambrian periods (Gallet et al., 2000, 2012; Elston et al., 2002; Pavlov and Gallet, 2010). Moreover, several superchrons, i.e. long periods (> 20 Myr) when the geomagnetic field remained in the same polarity (e.g. Jacobs, 2001), were detected during the Precambrian (references above and Driscoll and Evans, 2016). Examples include a superchron of normal polarity called Maya dated around 1.0 Ga (Pavlov and Gallet, 2010; Gallet et al., 2012), one of reverse polarity at ~1.4 Ga ("Elsonian"; Elston et al., 2002) and another one of normal polarity at ~1.75 Ga ("Cleaver"; Irving et al., 2004).

The dichotomy between periods marked by frequent reversals and superchrons, with seemingly abrupt transitions between them (see also Gallet and Pavlov, 2016), led Gallet et al. (2012) to propose an evaluation of the frequency of superchrons during the Precambrian (Pavlov and Gallet, 2010; Driscoll and Evans, 2016), which amounts to studying magnetic reversal frequencies averaged over very long time intervals. Following Wicht et al. (2011), Gallet et al. (2012) suggested that a higher superchron frequency might be linked to a higher sensitivity of the geodynamo before the growth of the inner core to the prevailing thermal conditions at the core-mantle boundary. However, Driscoll and Evans (2016) recently suggested the frequency of superchrons has remained constant over the past two billion years. The difficulty of validating such analyses stems from a small number of reliable Precambrian magnetostratigraphic data. On this issue, several sedimentary sections located in Siberia have yielded detailed magnetic polarity sequences thanks to a remarkable preservation of the magnetization acquired during their deposition (Gallet et al., 2000, 2012; Pavlov and Gallet, 2010).

In the present study, we further extend the existing Precambrian magnetostratigraphic data by providing new results obtained from several sedimentary formations of the Turukhansk Uplift region. Ultimately, we seek to better document the Maya superchron at the ~1 Gyr-old transition between the Mesoproterozoic and the Neoproterozoic.

2. Geological setting and age constraints on the Turukhansk Uplift succession

The Turukhansk Uplift region is a tectonic structure that is approximately ~130 × 30 km wide. It is located on the right bank of the Yenisey River along the north-western margin of the Siberian craton (Fig. 1a; e.g. Semikhatov and Serebryakov, 1983; Petrov and Semikhatov, 2001; 2009). In this ~4.5 km-thick structure, a late Meso- to early Neoproterozoic succession comprising successively the Bezymyanny, Linok, Sukhaya Tunguska, Derevnya, Burovaya, Shorikha, Miroedikha and the Turukhansk formations occurs in three north-south trending and reverse fault-bounded tectonic blocks. These blocks were thrust upon the western margin (in modern coordinates) of the Siberian platform, onto Ediacaran (Upper Vendian) and Paleozoic strata, during the middle Paleozoic (Mikutskiy and Petrakov, 1961, Kravtsov, 1967) or the Triassic (Nikishin et al., 2010). Two blocks, an eastern one called Golyi Yar and a central one referred to as the Turukhansk block, dominate the overall Turukhansk structure. In contrast, a western block called Durnoi Mys outcrops in a limited area near the mouth of the Nizhnyaya Tunguska River (N. Tunguska; Fig. 1b). The main faults are separated by a second-order transverse to diagonal strike-slip fault system, which played a major role in the tectonic evolution of the Miroedikha fault zone and of the northern part of the Turukhansk block.

The different blocks predominantly encompass gentle (~15°–35°) westward-dipping (~250°–280°) homoclines, with local complexities due to small near-fault anticlines. An asymmetrical syncline is found in the western periphery of the Turukhansk block. All limbs are partly faulted in this large-scale tectonic region with gently dipping limbs to the east and subvertical limbs to the west.

The Golyi Yar block is in the Eastern part of the region, with its southern part lying along the Sukhaya Tunguska River. Since the regional tectonic squeezing increases westward, the Golyi Yar block is tectonically the least disturbed area. In contrast, most deformations occur in the narrow Miroedikha zone and in the northern part of the Turukhansk block along the Bolshaya Shorikha River. In the northern Turukhansk block, the homocline dip increases up to ~40° and the orientation of the structures appears rotated by ~25° counterclockwise relative to the central zone. The intensive tectonic stress results in dolomitized rocks, small-scale tectonic deformations and fractures, with breccia-like veins and a zebra texture within the carbonate series. Similar sucrosic-type dolomites occur locally as discrete white patches along faults in the central zone of the Turukhansk block that is close to the N. Tunguska river.

Meso- to Neoproterozoic Turukhansk deposits are overlain with an angular unconformity by near-horizontal Ediacaran (Upper Vendian) to Cambrian strata of the Platonovskaya Formation. The whole Turukhansk section is divided into two internally continuous successions by a single stratigraphic hiatus at the base of Derevnya Formation (Fig. 1c). Based on microfossil and stromatolite assemblages (Semikhatov and Serebryakov, 1983; Petrov and Veis, 1995; Sergeev, 2006) and chemostratigraphic data (Bartley et al. 2001), this boundary corresponds with the base of the Upper Riphean, which has been dated to ca 1030 Ma (Semikhatov et al., 2000). This dating is supported by an isochron Pb–Pb age of 1035 ± 65 Ma obtained from the underlying limestones of the Sukhaya Tunguska Formation (Ovchinnikova et al., 1995). A description of the Pb-Pb dating method and a discussion of its reliability and accuracy can be found in Kaurova et al. (2010) and Kuznetsov et al. (2017) (and references therein). K–Ar and Rb–Sr ages of ca 850 Ma obtained from glauconite minerals from multiple stratigraphic levels of the Turukhansk section may correspond to a time of regional meteoric catagenesis (Gorokhov et al., 1995). On this assumption, and further considering Carbon and Strontium-isotope stratigraphy and regional correlation data (Knoll et al., 1995; Khudoley et al., 2007), a minimum depositional age of the Turukhansk section is estimated at ca 850–900 Ma, before the beginning of regional uplift and erosion.

There are several lines of evidence, relying on lithological, paleontological, geochronogical, chemostratigraphic and paleomagnetic data, that indicate a close correlation between the Riphean sequences from the Turukhansk Uplift and the Uchur-Maya regions, the latter being located in southeastern Siberia (e.g. Semikhatov and Serebryakov, 1983; Bartley et al., 2001; Gallet et al, 2000; Khudoley et al., 2007). In this correlation frame, the sequence spanning from the Linok Formation to the Turukhansk Formation in the Turukhansk region is nearly coeval to that ranging from the Totta Formation to the Ust-Kirba Formation of the Uchur-Maya region, including the Malgina Formation (1043 ± 14 Ma; Ovchinnikova et al., 2001) and the Lakhanda Group (~1025–930 Ma; Semikhatov et al., 2000; Khudoley et al., 2007).

In this study, we report new paleomagnetic data obtained from the Linok, Sukhaya Tunguska, Derevnya, Burovaya and Turukhansk formations (Fig. 1c). The Linok Formation is a clayey-carbonate succession lying between the siliciclastic Bezymyanny and the carbonate Sukhaya Tunguska formations at the base of the Riphean sedimentary sequence (Petrov, 2000). This Formation is subdivided into three parts: the lower (~18–45 m) clayey-calcareous, middle (~40–75 m) argillite-dominated, and upper (~120–220 m) carbonate sub-formations (Fig. 2). According to Petrov (1993), grey to dark-grey rocks from the lower and middle sub-formations of the Linok Formation correspond to the aggradational development of the distal and relatively deep part of the basin with mixed clayey-calcareous sedimentation. The upper sub-

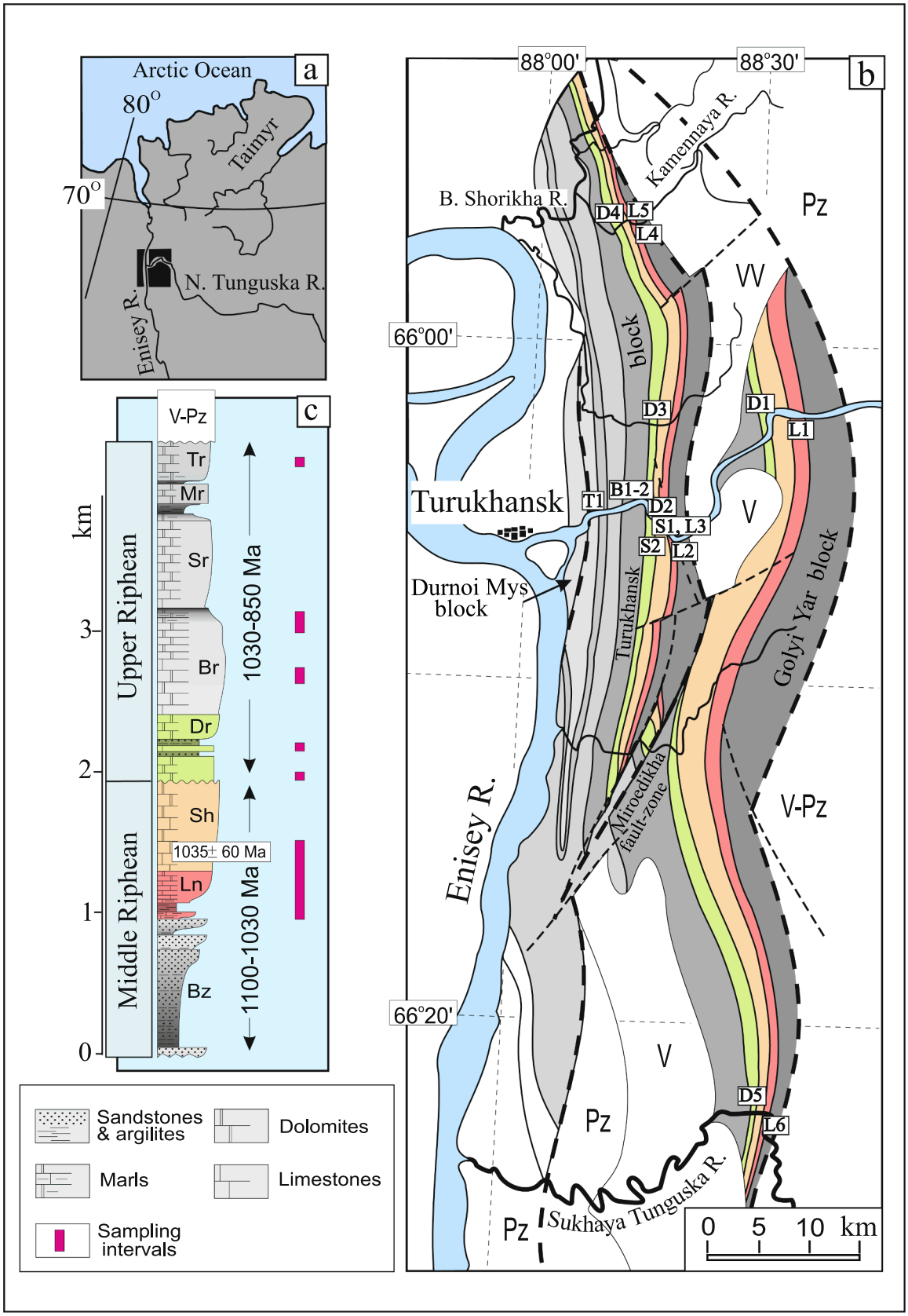

Fig. 1. (a) Location of the Turukhansk region along the northwestern margin of the Siberian platform. (b) Geological map of the Turukhansk Uplift. The sections from the Linok, Sukhaya Tunguska, Derevnya, Burovaya and Turukhansk formations analyzed in the present study are labeled L1 to L6, S1 and S2, D1 to D5, B1 and B2, and T1 respectively. See description in the text. (c) Simplified lithological and age description of the Middle and Upper Riphean formations of the Turukhansk Uplift. Bz, Bezymyanny Fm.; Ln, Linok Fm.; Sh, Sukhaya Tungunska Fm.; Dr, Derevnya Fm.; Br, Burovaya Fm.; Sr, Shorikha Fm.; Mr, Miroedikha Fm.; Tr, Turukhansk Fm. V-Pz refers to Vendian to Paleozoic deposits.

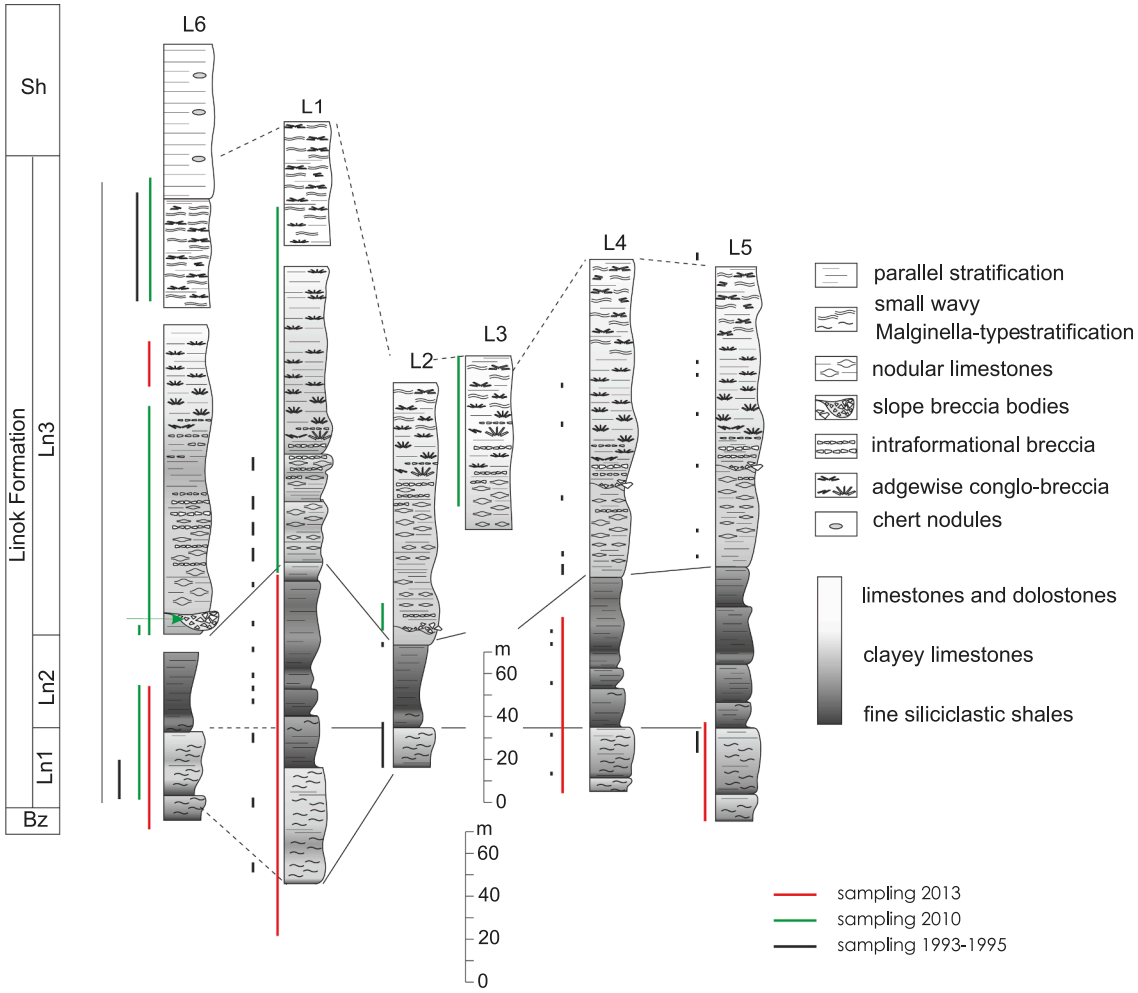

Fig. 2. Lithological description of the different sections of the Linok Formation analyzed in the present study. The stratigraphic spread of the magnetostratigraphic sampling is further indicated to the left of each lithological sequence (see color code on the figure). (For interpretation of the references to color in this figure legend, the reader is referred to the web version of this article.)

formation, with generally light-grey colored rocks, reflects the formation and expansion processes of the carbonate platform.

The Sukhaya Tunguska Formation ends the large terrigenous–carbonate sedimentary cycle observed in the lower part of the Riphean sequences of the Turukhansk Uplift (Petrov, 1993). This unit is a thick (530–670 m) sequence of dark colored limestones, which progressively evolve toward mostly pale-colored dolomites (Sergeev, 2006). The top of the Sukhaya Tunguska Formation is marked by a regional discontinuity, and is overlain by stromatolitic dolomites of the Derevnya Formation (Semikhatov and Serebryakov, 1983; Petrov and Veis, 1995).

The Derevnya Formation consists of mixed stromatolite and siliciclastic shelf deposits divided into lower (~35–105 m) carbonate, middle (~80–100 m) carbonate-siliciclastic and upper (~60–70 m) carbonate members (Petrov and Semikhatov, 2005). The lower and middle members contain variegated red-colored dolomites and diverse stromatolite assemblages.

The 600–1000 m-thick Burovaya Formation is a reef-bearing carbonate unit, which rests conformably on the clayey-carbonate Derevnya Formation, whereas it is disconformably overlain by the basal siliciclastic package of the carbonate-dominated Shorikha Formation. A distinctive erosional surface separates the Burovaya Formation into two subformations. The lower subformation constitutes a single facies complex composed of dark colored, fine-grained limestones and dolostones with subordinate stromatolitic and intraclastic carbonates. The upper subformation comprises two facies complexes. The lower, reef-bearing complex consists of light grey stromatolitic dolostones and limestones up to 550 m thick, surrounded by 220–400 m of dark grey, predominantly fine-grained carbonates. The upper ~130 m-thick complex, consisting of clayey carbonates and subordinate shales, conformably overlies the preceding reefal and peri-reefal sediments.

Finally, the Turukhansk carbonate Formation is the uppermost unit of the Riphean sequence in the Turukhansk region (Fig. 1c). With a thickness of 160–200 m, it comprises pink-reddish and pale-grey clayely dolomites, stromatolitic dolomites and intraclastic beds.

Based on petrographic and mineralogical data, the deposits above show no evidence for low-grade metamorphic effects. The Sukhaya Tunguska carbonate strata contain well-preserved micrite-dominated peloidal structures with excess-calcium dolomite associated with specific combinations of authigenic phyllosilicates, that are unstable under deep burial conditions (Petrov, 2016). Siliciclastic strata of the Derevnya Formation contain authigenic Fe-kaolinite cement (Petrov and Semikhatov, 2005). Moreover, the light color and the high quality of preservation of the Derevnya acritarchs further suggest an insignificant degree of kerogen alteration, the latter being otherwise expected under burial conditions (Petrov and Veis, 1995).

3. Sampling and methods

During two field seasons in 2010 and 2013, we conducted a relatively dense sampling of six sections (L1–L6) across the Linok Formation. The sampling consisted in collecting along the stratigraphy

Fig. 3. Photos of three sampled sections of the Linok and Burovaya formations (@ Y. Gallet). (a) Middle part of Linok Section L1. (b) Middle part of Linok Section L6. (c) Burovaya Section B1.

hand samples oriented using a magnetic compass. The sections are in different parts of the Turukhansk region (Fig. 1). The two sections referred to as L1 and L6 were sampled in the easternmost block along the Nizhnyaya Tunguska and the Sukhaya Tunguska rivers, respectively. They encompass the entire Linok Formation (Figs. 1–3). There is only one significant stratigraphic gap of ~20 m around the upper part of the intermediate sub-formation (Ln2, Section L6; Fig. 2). Sections L2 and L3 are both located in the central block, along the Nizhnyaya Tunguska river (Fig. 1). Together, they contain most of the upper Linok sub-formation (Ln3; Fig. 2). Finally, the sections L4 and L5 also stand in the central block, along the Kamennaya river for the first section and along its tributary Pravyi creek for the second. The data mainly documents the lower and intermediate Linok sub-formations (Figs. 2 and 3). Linok section sampling was performed in stratigraphic order, with a spacing ranging from ~0.3 to ~2 m depending on the quality of exposure. The sections have different dipping attitudes, offering the possibility to make a fold test. Furthermore, a conglomerate level situated at the base of the upper Linok sub-formation was sampled in section L6 (Fig. 2). In total, more than 1200 hand samples were collected from the different Linok sections.

In September 2017, we additionally collected series of samples from the Sukhaya Tunguska, Burovaya and Turukhansk formations outcropping in the valley of the Nizhnyaya Tunguska river (Fig. 1). For the Sukhaya Tunguska Formation, 112 samples over a total stratigraphic thickness of about 200 m were collected first in a section located on the right bank of the river (S1), and next on its left bank in direct stratigraphic continuity (section S2). The sampling of the Burovaya Formation was conducted along the right bank of the Nizhnyaya Tunguska river from two sections with thicknesses of ~80 m and ~190 m-thick, respectively (referred to as B1 and B2; Fig. 1). These two sections belong to the upper part of both the upper (B1) and lower (B2) Burovaya subformations (see above). A total of 134 samples were collected in stratigraphic order, with a spacing of 0.8–2.5 m. Sampling of the Turukhansk Formation concerns a ~40 m-thick section (T1, Fig. 1) exposed on the right bank of the Nuzhnyaya Tunguska river, several kilometers upstream from the city of Turukhansk. It comprises a series of 44 samples collected in stratigraphic order with various spacing.

In the present study, we also re-analyzed thermal demagnetization data previously obtained from the Derevnya Formation by Pavlov et al. (2015). These data come from four sections referred to as D1–D4 (Fig. 1). We further report on new data from a fifth section (D5; Fig. 1). The sampling of the Derevnya Formation was concentrated on a single stratigraphic interval of several meter-thick red colored carbonates in each section, with a collection of 15–30 samples in each one. Whereas the rocks sampled in section D1 are from the lower part of the Derevnya Formation, those from sections D2, D3, D4 are from its middle part. The stratigraphic position of reddish stromatolites corresponding to section D5 is unclear for both the lower and the middle part of the Derevnya Formation. Hereafter, we will consider each Derevnya outcrop as a single paleomagnetic site.

In the laboratory, the hand samples were cut into cubic specimens (8 cm^3). All paleomagnetic measurements were carried out using a 2G cryogenic magnetometer housed in a magnetically shielded room both at the Institut de Physique du Globe de Paris and at the Institute of Physics of the Earth-Russian Academy of Sciences (Moscow). The samples were thermally demagnetized in 13 to 18 steps and the directions of the magnetization components were determined via principal component analyses (Kirschvink, 1980) using the PaleoMac software (Cogné, 2003). Rock magnetic analyses were also performed with the aim to further constrain the magnetic mineralogy of the samples.

4. Paleomagnetic analyses

In this section, the thermal demagnetization data obtained from the Linok, Sukhaya Tungunska, Derevnya, Burovaya and Turukhansk formations are successively presented. It is worth noting that the new data from the Linok and Sukhaya Tunguska formations rely on a much larger collection of samples than that previously analyzed by Pavlov and Petrov (1996), Gallet et al. (2000) and Pavlov et al. (2015), while no result was available until now for both the Burovaya and Turukhansk formations.

a) LK690, L1 /Ln1-2

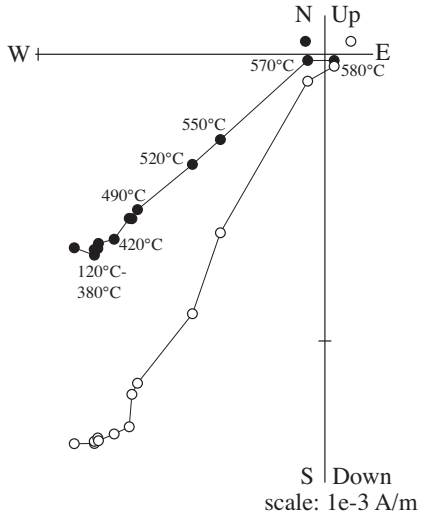

b) LK61, L1 /Ln1-2

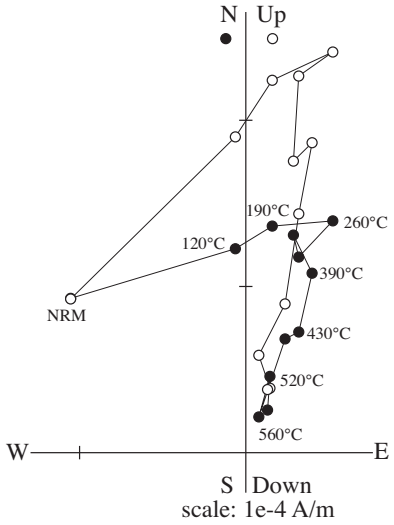

c) LK655, L2 /Ln3

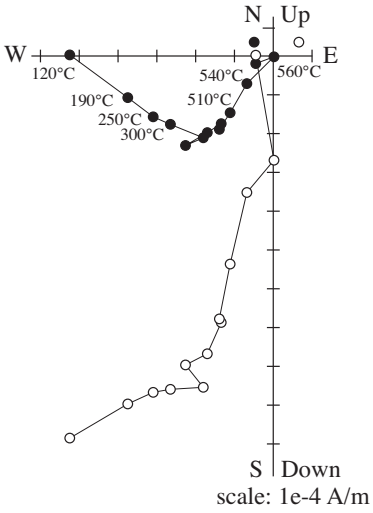

d) LK728, L3 /Ln3

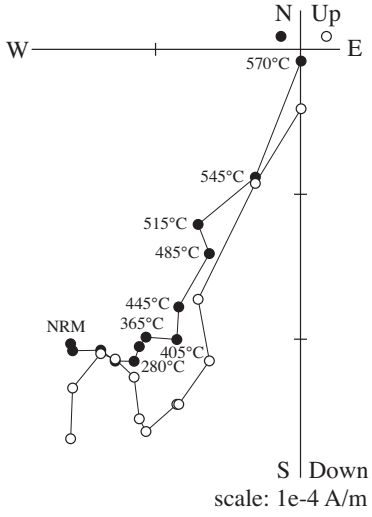

e) LK184, L4 /Ln1-2

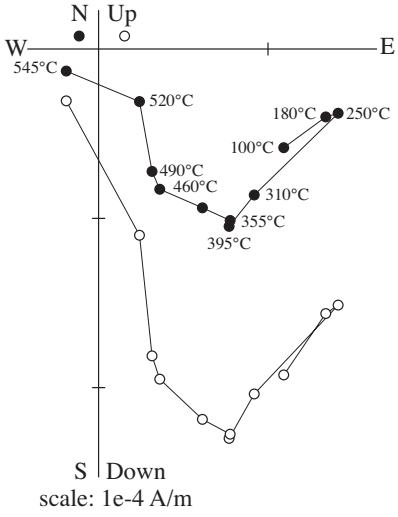

f) LK237, L5 /Ln1-2

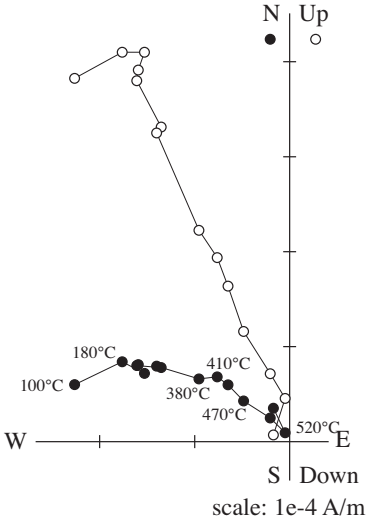

g) LK267, L5 /Ln1-2

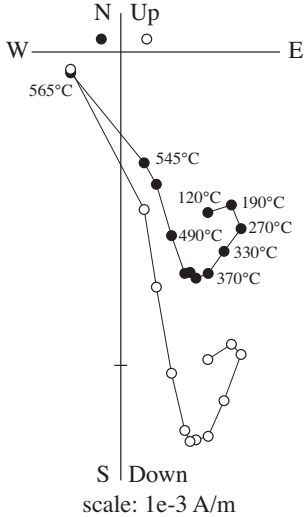

h) LK306, L6 /Ln1-2

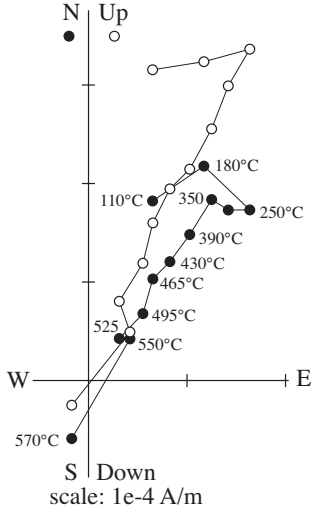

i) LK536, L6 /Ln3

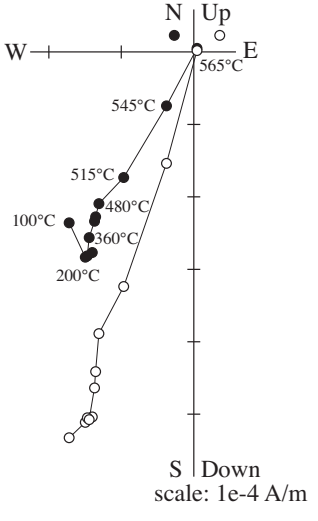

(caption on next page)

Fig. 4. Orthogonal diagrams of progressive thermal demagnetization of samples from the Linok Formation. Solid (open) circles are in the horizontal (vertical) plane. All diagrams are in stratigraphic coordinates.

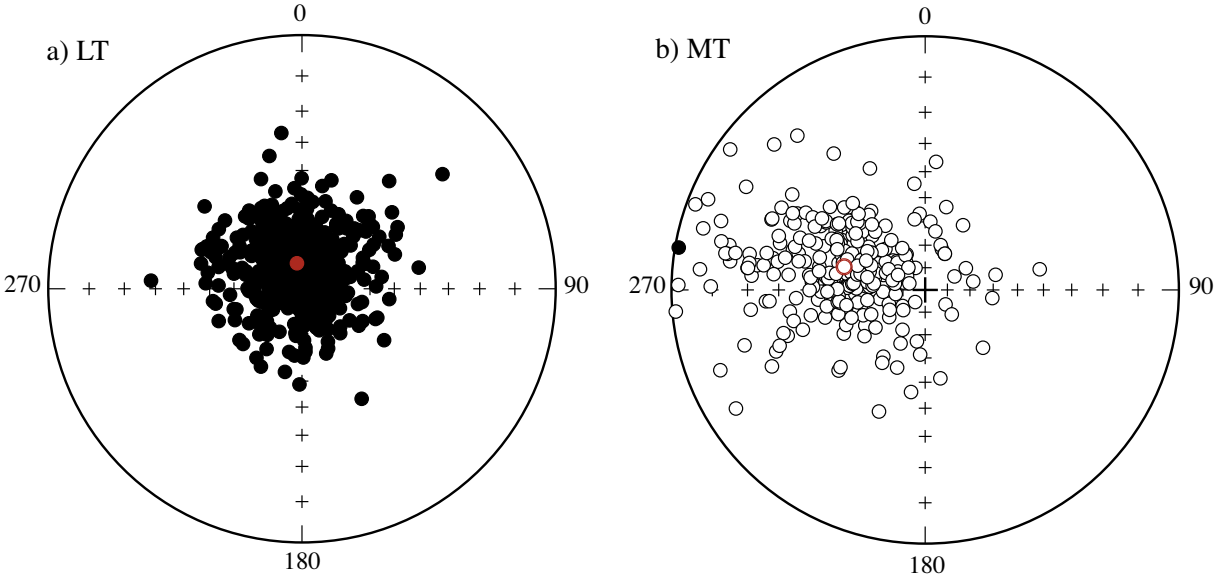

Fig. 5. Stereographic projection of all the directions isolated at the sample level in the Linok Formation over the low (a) and intermediate (b) unblocking temperature ranges (LT and MT components, respectively). All directions are reported before bedding correction.

4.1. Linok formation

Representative examples of thermal demagnetization diagrams from the Linok Formation are shown in Fig. 4. In general, the thermal treatment isolated three successive magnetization components. A first component is observed during the first two or three demagnetization steps, until about 200 °C. In geographic coordinates, this component (LT) has a similar direction to the present-day field at the sampling sites (Fig. 5a). We therefore consider that it likely represents a recent overprint with a viscous origin. Next, a magnetization component with always the same magnetic polarity is isolated in the temperature range between ~200 °C and ~400–450 °C (hereafter referred to as MT; Figs. 4 and 5b). A high unblocking temperature component (HT) is finally observed until the total demagnetization of the samples, which is achieved at approximately 550–580 °C. This component unambiguously possesses two magnetic polarity states (Fig. 6).

The demagnetization data clearly show that the magnetization of the Linok samples is mainly carried by minerals from the (titano) magnetite family (see also Gallet et al., 2000). In a few cases, there is also evidence for the presence of a mixture of both magnetite and hematite. This is further confirmed by the thermal demagnetization of isothermal remanent magnetization (IRM) acquired along three perpendicular directions in fields of 1.8 T, 0.2 T and 0.05 T (Lowrie, 1990; Fig. S1a,b in Supplementary material).

4.2. Sukhaya Tungunska Formation

The thermal demagnetization of the samples from sections S1 and S2 of the Sukhaya Tunguska Formation is achieved at relatively low temperatures, around 470–500 °C (Fig. 7), indicating that their magnetization is predominantly carried by minerals from the (titano) magnetite family (Fig. S1c,d in Supplementary material; note that a non-negligible fraction of high-coercivity minerals is also present). The LT component with a steep inclination in geographic coordinates is removed in the first demagnetization steps. For some samples, however, this component may persist until the end of the demagnetization, which suggests their total remagnetization in the recent field. Several samples distinctly show the same MT component previously observed in the Linok Formation (Fig. 7a, b and e). A strong overlap between the LT and MT components leads in rare cases to an apparent component pointing toward the north-west with a positive inclination both in geographic and stratigraphic coordinates, which in fact has no geomagnetic meaning. Several demagnetization diagrams also clearly indicate the presence of a supplementary component pointing towards the North-East, but the latter remains ill-defined because of its strong overlap with the MT component (Fig. 7c and d).

4.3. Derevnya Formation

Thermal demagnetization of samples from the Derevnya Formation reveals the same succession of three magnetization components as that observed for the Linok Formation (Fig. 8). The LT component with a direction in geographic coordinates parallel to that of the present-day field is isolated up to ~200 °C, the MT component similar to that from the Linok Formation is isolated up to 450 °C, and lastly, the HT temperature component is evidenced up to 620–680 °C (Fig. 8a and b). The HT component consistently shows the same magnetic polarity (Fig. 8c–g). These data and those provided by the thermal demagnetization of 3-axis IRM (Fig. S1e,f in Supplementary material) clearly indicate that the magnetic mineralogy of the Derevnya samples contains both magnetite and hematite, with a predominance of hematite.

4.4. Burovaya Formation

The thermal demagnetization data from samples of the Burovaya Formation show a behavior rather different between the two sections B1 and B2. The data from section B1 yield a paleomagnetic behavior characterized by three successive magnetization components similar to that previously described for the Linok and Derevnya formations (Fig. 9a and b). The MT component is particularly well developed and in some cases, its unblocking temperature range largely overlaps that of the HT component (Fig. 9f). Nevertheless the HT component, showing a single polarity state, is confidently isolated in most samples, until the end of the demagnetization achieved at ~575 °C. (Fig. 9g). This

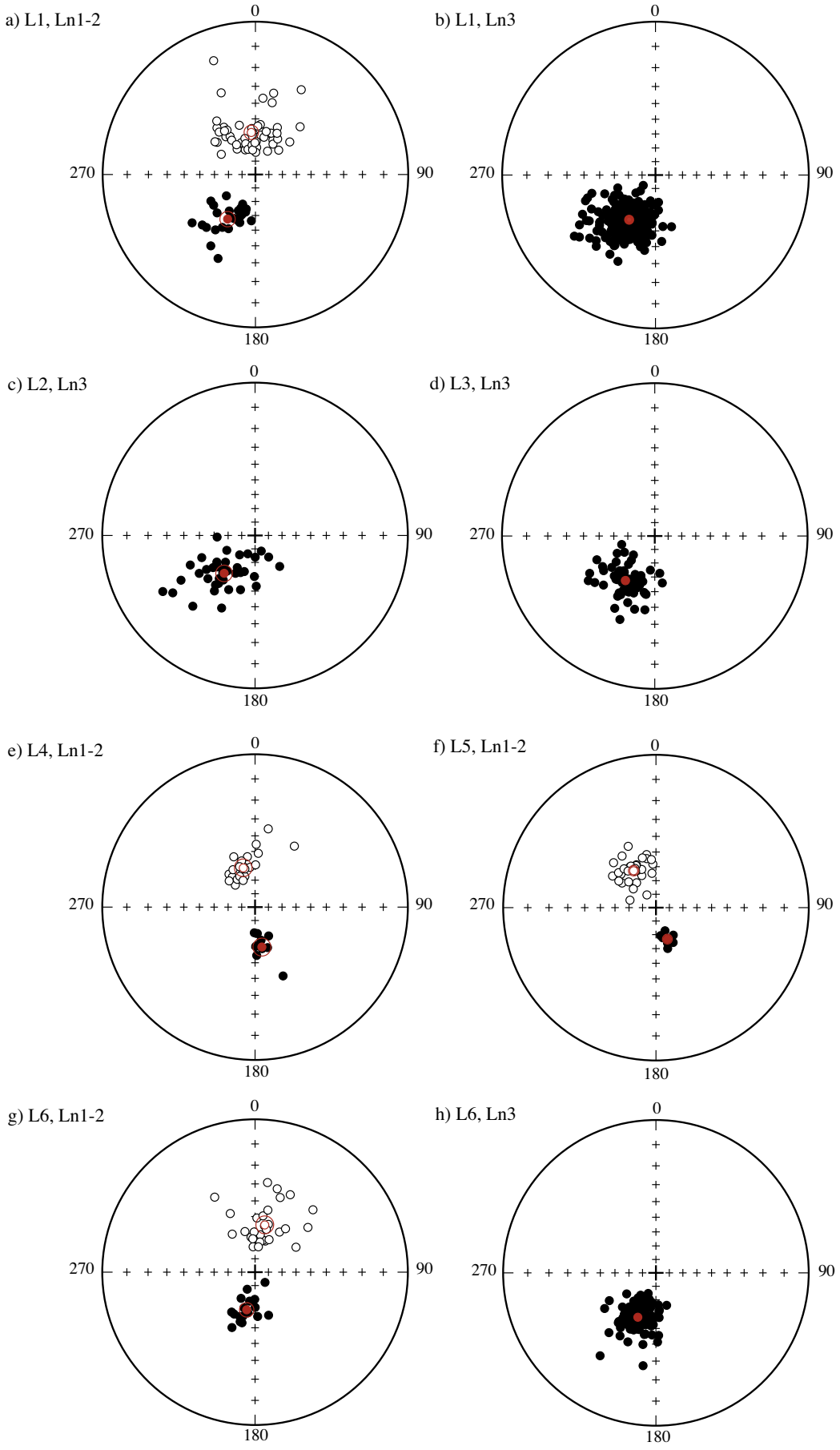

(caption on next page)

Fig. 6. Stereographic projection of the normal and reversed polarity directions of the high unblocking temperature magnetization component isolated in the different sections of the Linok Formation. All data are reported after bedding correction. Whenever possible, the directions obtained from the lower (Ln1) and middle (Ln2) sub-formations were distinguished from those of the upper sub-formation (Ln3). The averaged directions estimated for each polarity state are shown in red. (For interpretation of the references to color in this figure legend, the reader is referred to the web version of this article.)

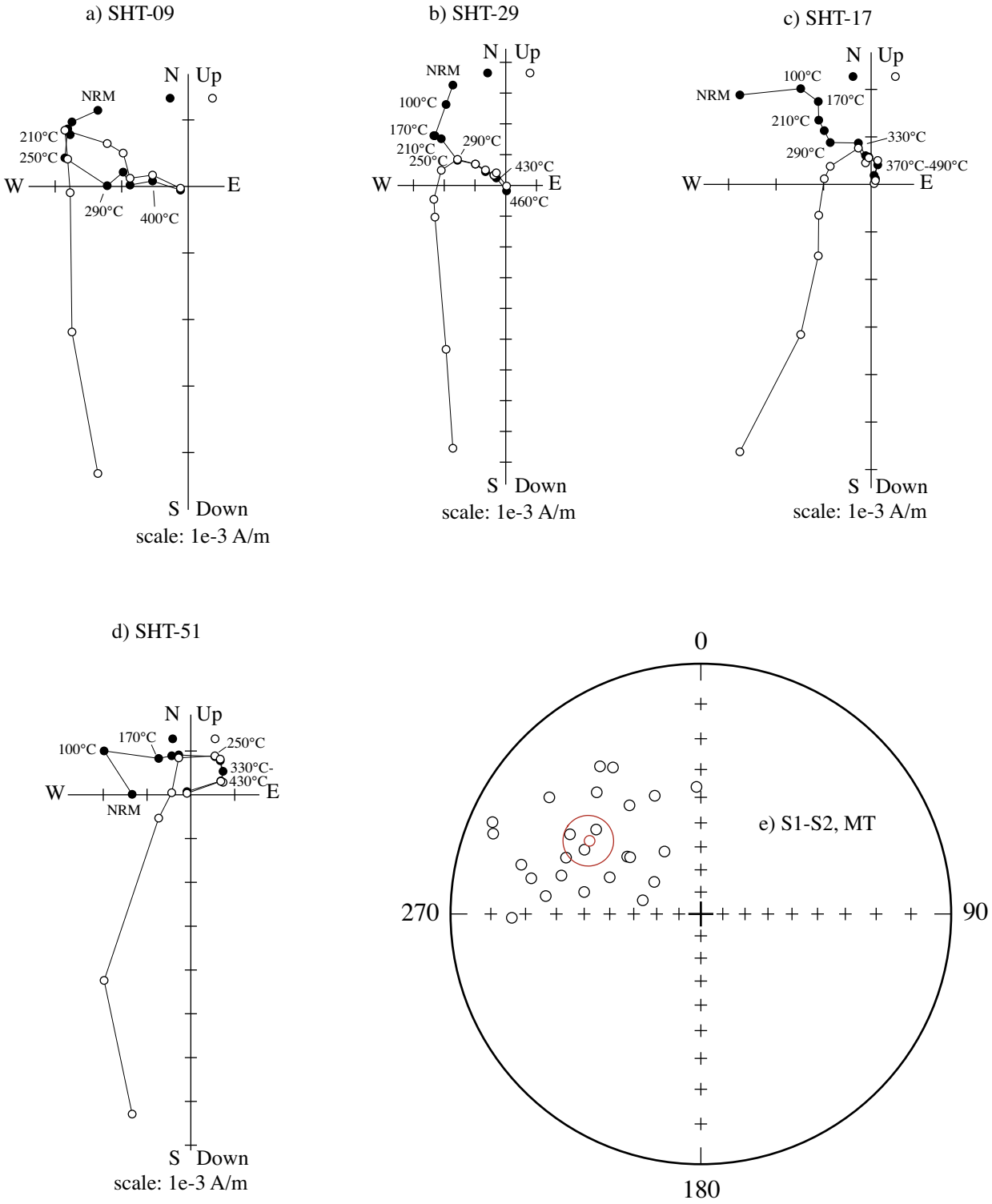

Fig. 7. Demagnetization data and directions obtained from the Sukhaya Tunguska Formation. (a)–(d) Four examples of orthogonal diagrams of progressive thermal demagnetization in geographic coordinates. Solid (open) circles refer to the horizontal (vertical) plane. (e) Stereographic projection of the directions before bedding correction of the MT magnetization component isolated both in Section S1 and S2.

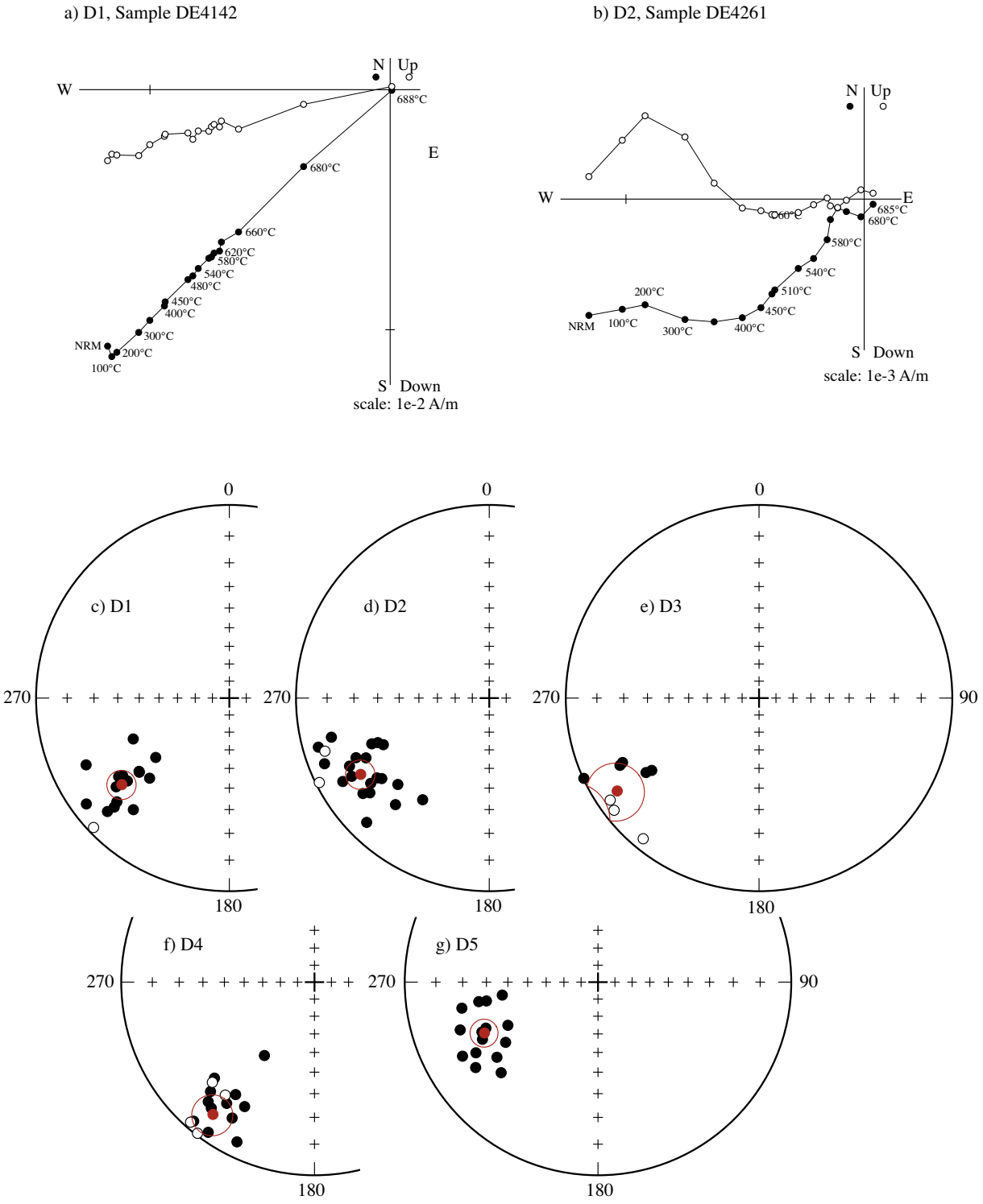

Fig. 8. Demagnetization data and directions obtained from the Derevnya Formation. (a) and (b) Two examples of orthogonal diagrams of progressive thermal demagnetization in stratigraphic coordinates. Solid (open) circles refer to the horizontal (vertical) plane. (c)–(g) Stereographic projection of the directions of the high unblocking temperature magnetization (HT) component isolated in the different sections of the Derevnya Formation. All data are reported after bedding correction. For each section, the averaged direction is shown in red. (For interpretation of the references to color in this figure legend, the reader is referred to the web version of this article.)

maximum unblocking temperature clearly indicates that magnetite is the main carrier of the magnetization in these samples (see also Fig. S1g,h in Supplementary material).

Up to four magnetization components are distinguished in samples from section B2 (Fig. 9c–e). The LT component having the present-day field direction is isolated until ~220 °C. The MT component is present, but in very weak proportion relative to the total magnetization. The determination of its direction is not possible because of significant overlap either with the LT component or with the component isolated at higher temperature (above 350 °C). Next, a magnetization component is accurately isolated up to 500–525 °C (Fig. 9h). It is important to note that the samples are totally demagnetized at this temperature and their

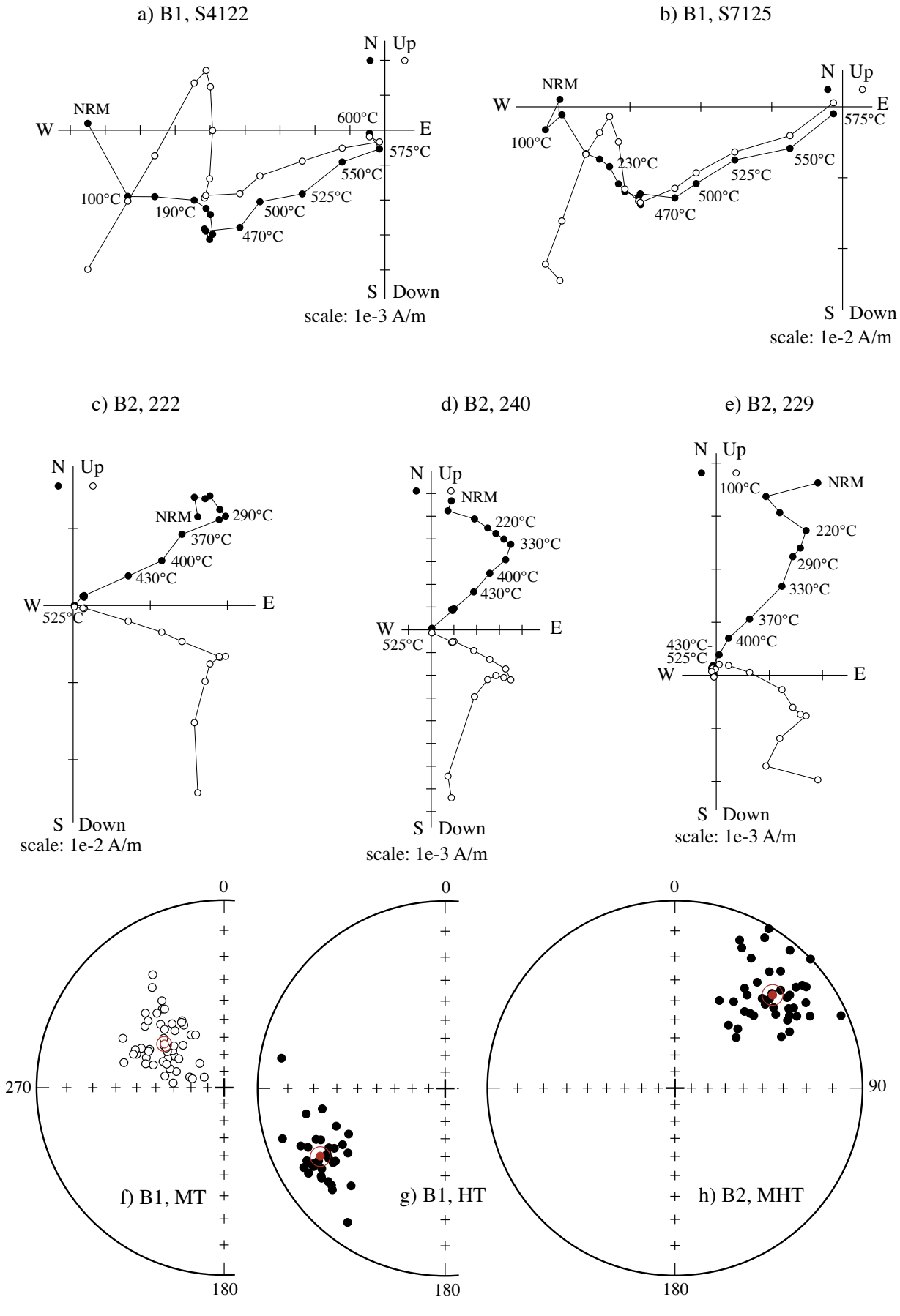

(caption on next page)

Fig. 9. Demagnetization data and directions obtained from the Burovaya Formation. (a) and (b) and (c)–(e) Examples from Section B1 and Section B2 of orthogonal diagrams of progressive thermal demagnetization. All these diagrams are reported in stratigraphic coordinates. Solid (open) circles refer to the horizontal (vertical) plane. (f) Stereographic projection of the directions before bedding correction of the MT magnetization component isolated in Section B1. (g) Stereographic projection of the directions in stratigraphic coordinates of the HT magnetization component obtained in Section B1. (h) Stereographic projection of the directions after bedding correction of the MHT magnetization component isolated in Section B2.

magnetic mineralogy appears very similar to that observed in the samples from the Sukhaya Tungunska Formation (Fig S1i,j in Supplementary material). For most samples, the middle-high unblocking temperature component goes straight to the origin of the demagnetization diagrams (Fig. 9c and d). However, a fourth component is distinguishable in some cases but it is never accurately isolated because of overlap of its unblocking temperature spectrum with that of the previous component (Fig. 9e).

4.5. Turukhansk Formation

Thermal demagnetization of the samples from the Turukhansk Formation allows one to strengthen the magnetic behavior previously observed in samples from the section B2 of the Burovaya Formation. The data clearly isolate four successive magnetization components, with this time the HT component precisely defined (Fig. 10a–d). The LT and MT components, being the same as before, are recognized (Fig. 10e), as well as the component observed in the Burovaya Formation over the same unblocking temperature range (i.e. up to ~500 °C) either as a final or an intermediate component (Fig. 10f). Hereafter, this component is referred to as MHT. Finally, the HT magnetization component is isolated up to 660–680 °C, which indicates that it is carried by hematite, while the fraction of low-coercivity minerals is very weak (Fig S1k,l in Supplementary material). This component possesses the two magnetic polarities, with a single reversal found within the sampled stratigraphic sequence (Fig. 10g).

5. Interpretation of the magnetization components

Four magnetization components called LT, MT, MHT and HT were isolated from our collection of samples. The LT component, which shows in geographic coordinates the direction of the present-day field at the sites, is not discussed further.

5.1. MT component

The MT component is consistently observed in all the studied formations of the Turukhansk Uplift region, even though its direction cannot always be precisely determined because of overlaps with other components. In geographic coordinates, the directions determined for this component point toward the west and show negative inclinations (Fig. 11a; Table S1). After averaging these directions at the level of each section, the fold test deriving from that proposed by McElhinny (1964) conducted on the MT component is negative (Ks/Kg = 0.5), thus indicating a post-folding acquisition. However the use of the more sophisticated fold test designed by Shipunov (1997) indicates that the MT component might have a synfolding age (Table S1). Whatever the case, the mean MT paleomagnetic pole estimated from all samples (or from the different sections) appears in very good agreement with secondary magnetization previously isolated in Early and Middle Paleozoic rocks from the southern, southwestern and northwestern disturbed margins of the Siberian platform (e.g. Bachtadse et al., 2000; Shatsillo et al., 2012 and unpublished data). We speculate that the MT component was acquired during the Carboniferous period, i.e. in relation with tectonic events at the final stage of the closure of the Ural-Mongol Ocean (Zonenshain et al., 1990). In each of these regions, the MT magnetization component consistently has the same polarity, which was likely reversed since the Siberian platform was in the northern hemisphere during that period. We suggest that it was acquired during the Kiaman Permo-Carboniferous reverse superchron.

5.2. MHT component

The MHT component is clearly evidenced from the samples of the Burovaya and Turukhansk formations (sections B2 and T1; Table 1). Isolated in the very same temperature range (< 525 °C), it points toward the north-east with a shallow inclination (in geographic coordinates; Fig. 11b). On average, the directions (always of the same polarity) that can be determined from the two series of samples are statistically distinct at the 95% confidence level in geographic coordinates ($\gamma/\gamma c = 17.1°/7.4°$; McFadden and McElhinny, 1990), whereas they are statistically identical in stratigraphic coordinates ($\gamma/\gamma c = 6.2°/7.4°$; Fig. 11c). This indicates that this component was likely acquired either before or at the earliest stage of the folding, which occurred before the deposition of the nearly unfolded Ediacarian to Lower Cambrian Platonovskaya Formation, thus during the Neoproterozoic. Note further that the corresponding paleomagnetic pole is different from all Phanerozoic poles of the Siberian platform (e.g. Torsvik et al., 2012).

It is also worth mentioning that the MHT component is most probably the third ill-defined component only glimpsed in some samples from the Sukhaya Tungiska Formation (Fig. 7c and d).

5.3. HT component

The different HT magnetization components (Table 1) are isolated up to unblocking temperatures close to the Curie temperature of magnetite (for the Linok and Burovaya-B1 formations) or to that of hematite (for the Derevnya and Turukhansk formations). We first focus on the primary origin of the HT component (i.e. syn-sedimentary) isolated in the Linok Formation, which is strongly constrained by several evidences listed below.

- The directions are reasonably well clustered (Table 1) and we used the McFadden and McElhinny (1990) reversal test to verify the antipodality between the normal and reverse data distributions. Fig. 6 shows that magnetic polarity reversals are only observed in the lower and intermediate Ln1 and Ln2 sub-formations, whereas the upper Ln3 sub-formation is always characterized by a single polarity. A positive reversal test is obtained for Ln1-Ln2 data from sections L4 and L6 ($\gamma/\gamma_c = 3.2°/10.5°$ and 6.9°/8.7°, respectively). However, the reversal test fails for sections L1 and L5 ($\gamma/\gamma_c = 22.2°/7.9°$ and 9.3°/7.3°, respectively). On the demagnetization diagrams, with quite often a significant overlap between the MT and HT components, we assume that the latter result is essentially due to a small bias in the determination of the HT directions caused by the MT component.
- A positive conglomerate test is obtained from the pebbles sampled in the lowermost part of the Ln3 sub-formation from section L6. The thermal demagnetization behavior of these samples is identical to that observed in samples from the undisturbed layers of the section (Fig. S2 in Supplementary material). The directions determined for the HT component are randomly distributed ($R/R_0 = 7.69/8.84$; Watson, 1956), which clearly indicates that the characteristic magnetization of the pebbles was acquired before the emplacement of the conglomerate layer.
- The mean HT directions estimated for the Ln1–Ln2 and upper Ln3 parts of sections L1 and L6 distinctly show the same trend towards

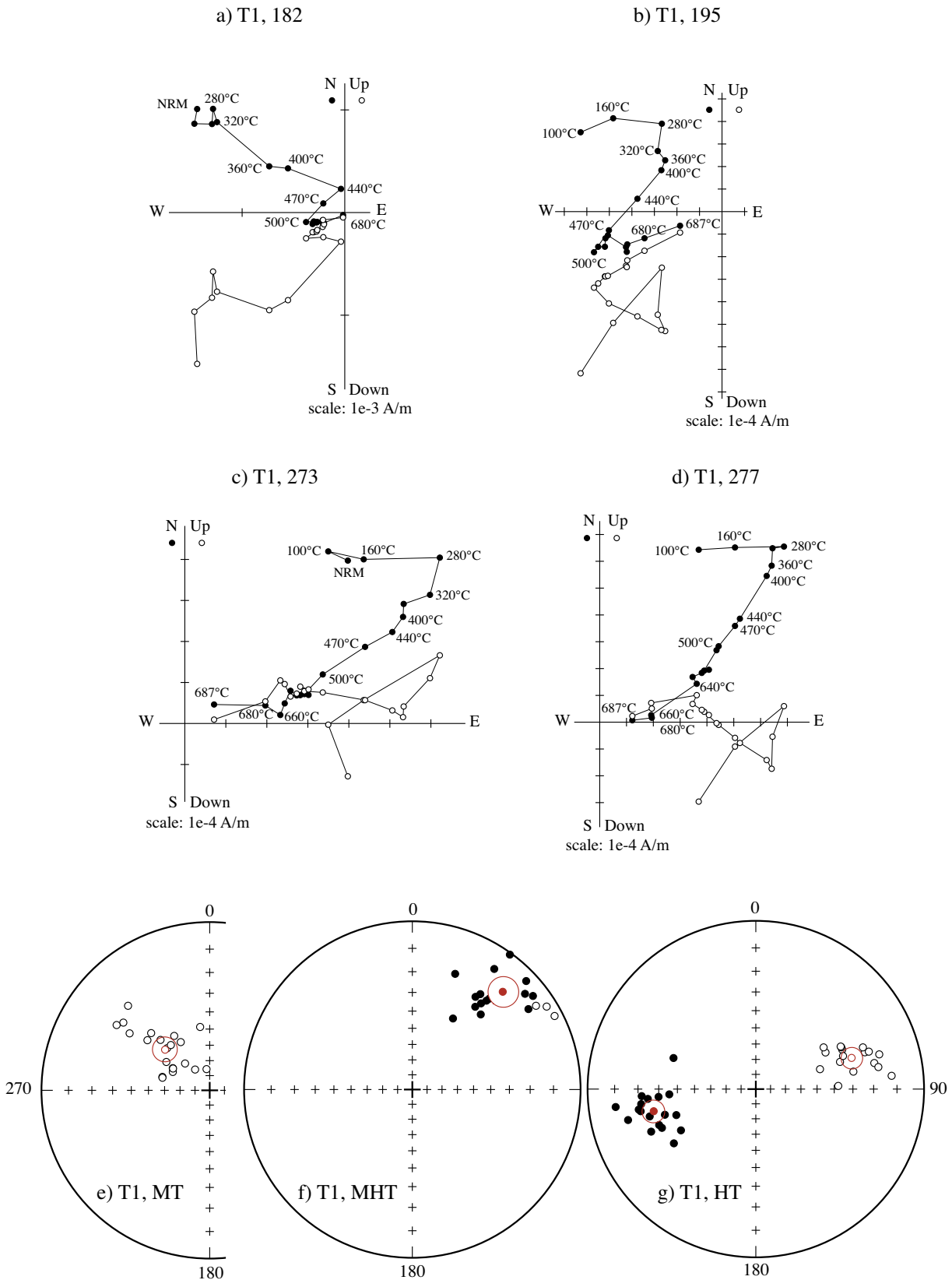

Fig. 10. Demagnetization data and directions obtained from the Turukhansk Formation. (a)–(d) Examples of orthogonal diagrams of progressive thermal demagnetization in stratigraphic coordinates. (e) Stereographic projection of the directions in geographic coordinates of the MT magnetization component. (f) and (g) Stereographic projection of the directions after bedding correction isolated for the MHT and HT magnetization components, respectively. The different mean directions are shown in red. (For interpretation of the references to color in this figure legend, the reader is referred to the web version of this article.)

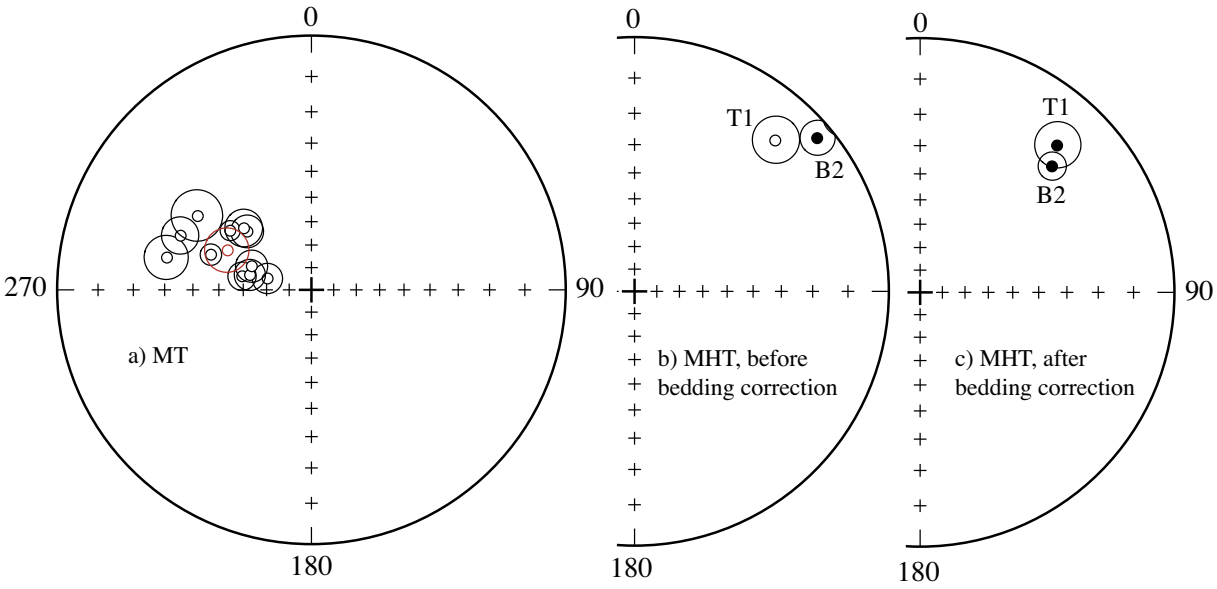

Fig. 11. Stereographic projections of the mean directions obtained at the section level for the MT and MHT magnetization components (Table S1). (a) Mean directions in geographic coordinates obtained for the MT component. (b),(c) Mean directions obtained for the MHT component before and after bedding correction, respectively. B2, T1: directions obtained from Section 2 of the Burovaya Formation and from the Turukhansk Formation, respectively.

the east (Fig. 12a; Table 1). The Ln3 directions are close to the directions of the same age obtained in Sections 2 and 3, and they also converge to the general mean HT direction determined for the overlying Derevnya and Burovaya formations. This feature suggests that, during their deposition, the sediments of sections L1 and L6 have recorded a motion of the Turukhansk block.

- The mean Ln1–Ln2 HT directions estimated from sections L4 and L5 are significantly different from those determined for sections L1 and L6. The angular difference is approximately 20° counterclockwise (Fig. 12b). A similar feature in HT direction is observed between section D4 and the other Derevnya sections (Fig. 12d). As sections L4, L5 and D4 are in the Turukhansk block region, which is further north than the other sections, the angular difference corresponds to the bend of the structures observed between the northern and southern parts of the Turukhansk block (Fig. 1). Therefore, the angular difference likely has a tectonic origin and the HT magnetization likely pre-dates this deformation, which is estimated to be from the Middle Paleozoic or Triassic age (see above).
- A fold test was carried out on the Ln1-Ln2 HT magnetization component obtained in sections L1 and L6, as well as on the Ln3 component isolated in sections L1, L2, L3 and L6. Although only two directions are considered for the Ln1 and Ln2 sub-formations, there is a strong grouping of these directions after tilt correction (Fig. 12e and f). Moreover, despite the relative rotation of 20° described above for sections L4 and L5, the inclusion of their HT directions leads to a positive fold test (Ks/Kg = 4.0; Enkin, 2003). A positive fold test was also achieved when the available mean Ln3 HT directions are considered (Ks/Kg = 15.9).

In contrast, the primary (early diagenetic) nature of the HT magnetization component found in the Derevnya Formation and in the first section of the Burovaya Formation is less well established from paleomagnetic tests. In both cases, this component does not exhibit geomagnetic field reversals and the fold test conducted by using the mean data from the different Derevnya sections is inconclusive (Ks/Kg = 1.2 without the mean HT direction obtained in section D4; Fig. 12c and d, Table 1). Nevertheless, strong arguments in favor of their primary origin rely on indirect evidences. First, the Derevnya and Burovaya HT directions are very similar and they are positioned in the continuity of the evolution observed between the Ln1-Ln2 and Ln3 HT directions from the underlying Linok Formation (Fig. 12a). Second, the paleomagnetic poles estimated for the Derevnya and Burovaya formation are different than all Phanerozoic poles obtained so far for the Siberian platform (e.g. Cocks and Torsvik, 2007). Third, the Derevnya and Burovaya paleomagnetic poles are consistent with the poles derived from the Lakhanda series and the Kandyk sills in the Uchur-Maya region assumed to be of similar ages (Fig. 13; e.g. Pavlov and Gallet, 2010 and see further discussion below).

Finally, the primary origin of the HT component isolated for the Turukhansk Formation relies on two main evidences. The first is that a positive reversal test ($\gamma/\gamma c = 7.5°/8.7°$) is obtained in stratigraphic coordinates between the mean directions of opposite polarity (Fig. 10g). The second is that its mean direction is relatively close to the HT directions obtained for the Derevnya and Burovaya formations (Fig. 12a). The corresponding paleomagnetic pole, which is again significantly different from all Phanerozoic Siberian poles, stands in the continuity of the directional trend drawn by the Linok, Derevnya and Burovaya paleomagnetic poles in agreement with that defined by the series of Meso-Neoproterozoic paleomagnetic poles obtained from the Uchur-Maya region (Fig. 13; see below).

6. Discussion

First, it is important to recall the difficulty in attributing a magnetic polarity to the directions of the HT magnetization component, which is isolated in the Linok, Derevnya, Burovaya and Turukhansk formations. This arises from a lack of comprehensive knowledge about the Apparent Polar Wander Path (APWP) of the Siberian platform between the Mesoproterozoic and Paleozoic periods. Following Pavlov and Gallet (2010) and Gallet et al. (2012), the polarity choice for the Late Mesoproterozoic relies on the hypothesis (which seems increasingly likely; e.g. Pavlov et al., 2015) that the north paleomagnetic pole was then situated in the Eastern hemisphere, within or close to the Indian Ocean area. In this case, the HT directions pointing toward the south/southwest with positive inclinations are of normal polarity. It follows that all the directions found in the upper part of the Linok Formation, in the different Derevnya sections and in the first section of the Burovaya Formation have a normal magnetic polarity.

Another issue concerns the complexity of the paleomagnetic signal recovered in several formations of the Turukhansk region. Our analyses

Table 1
Mean normal, reverse and/or normal + reverse paleomagnetic directions obtained for the middle-high (MHT) and high (HT) unblocking temperature magnetization components isolated before and after bedding correction in the different sections of the Linok, Sukhaya Tunguska, Derevnya, Burovaya and Turukhansk formations. N is the number of samples/sections used for the mean computations. Results of reversal test (γ/γ_c,), fold test (FT + for positive fold test) and derived paleomagnetic poles are also reported. The polarity option is discussed in the text.

Sections, coordinates, polarity (R,N)	N	In situ				Tilt corrected					
		D°	I°	K	α_{95}°	D°	I°	K	α_{95}°	Test	PLat°, PLon° dp°/dm°
FORMATION LINOK											
High temperature component Ln1-2											
L1, 65°56′ N, 88°31′E											
R	50	298.5	−49.2	13.9	5.6	354.1	−59.0	17.3	5.0		
N	24	162.9	66.1	8.6	10.7	212.3	52.3	34.3	5.1		
N + R	74	127.9	55.9	9.2	5.8	188.1	58.1	15.6	4.3	γ/γ_c = 22.2/7.9	
L4, 66°07′N, 88°00′E											
R	22	274.8	−36.1	20.3	7.0	344.0	−59.6	22.6	6.1		
N	10	92.8	36.1	34.3	8.4	169.7	61.0	60.3	6.3		
N + R	32	94.2	36.1	23.9	5.3	165.7	60.1	32.7	4.5	γ/γ_c = 3.2/10.5	
L5, 66°07′N, 88°10′E											
R	31	277.8	−27.8	43.1	4.0	328.3	−58.3	52.5	3.6		
N	8	90.1	35.5	248.8	3.5	160.8	65.6	248.8	3.5		
N + R	39	96.3	29.4	46.2	3.4	150.4	59.9	55.6	3.1	γ/γ_c = 9.3/7.3	
L6, 65°14′ N, 88°33′ E											
R	30	312.9	−27.6	16.4	6.7	11.6	−55.0	20.0	6.0		
N	17	128.4	32.4	24.1	7.4	192.5	61.9	50.7	5.1		
N + R	47	131.3	29.3	18.4	5.0	191.9	57.6	24.9	4.2	γ/γ_c = 6.9/8.7	
MEAN (for sections L1, L4, L5, L6)	4	111.2	38.9	16.4	23.4	174.6	60.0	65.4	11.4	FT+	
MEAN (for samples from sections L1 and L6)	121	129.6	45.3	9.0	4.5	189.6	57.9	18.4	3.1	FT+	Plat = 14.3 Plong = 80.8 dp/dm = 3.4/4.6
MEAN (for samples from sections L4 and L5)	71	95.4	32.4	31.2	3.1	157.3	60.2	39.2	2.7	FT+	
High temperature component Ln3											
L1											
N	219	187.4	60.8	33.5	1.7	210.2	51.9	33.5	1.7		
L2 65°48′N, 88°19′E											
N	39	137.9	42.7	18.5	5.5	218.9	55.0	17.6	5.6		
L3 65°49′N, 88°18′E											
N	78	177.9	62.7	28.2	3.1	213.0	51.8	33.8	2.8		
L6											
N	106	141.7	44.0	48.2	2.0	202.0	55.3	50.6	1.9		
MEAN	4	156.5	54.4	20.3	20.9	211.0	53.6	322.6	5.1	FT+	Plat = 12.5 Plong = 62.6 dp/dm = 5.0/7.1
FORMATION DEREVNYA											
High temperature component											
D1 65°56′ N, 88°30′E											
N	16	224.3	38.1	40.1	5.9	231.3	18.8	42.2	5.7		
D2 65°49′ N, 88°15′E											
N	22	233.2	27.6	26.0	6.2	239.4	14.3	33.3	5.5		
D3 65°55′ N, 88°16′E											
N	8	232.7	33.7	37.0	9.2	236.7	7.4	33.8	9.7		
D4 66°07′ N, 88°10′E											
N	16	209.9	36.8	41.1	5.8	217.6	8.1	29.2	6.9		
D5 65°15′ N, 88°31′E											
N	15	222.2	48.7	44.0	5.8	245.7	24.0	44.0	5.8		
MEAN (D1, D2, D3, D5)	4	228.5	37.1	66.8	11.3	238.2	16.2	80.6	10.3	FT?	Plat = −4.8 Plong = 30.8 dp/dm = 5.5/10.6
FORMATION BUROVAYA											
High temperature component											
B1 65°50′ N, 88°13′E											
N	39	234.0	35.3	44.1	3.5	241.2	14.6	42.5	3.6		Plat = −4.5 Plong = 27.6 dp/dm = 1.9/3.7
Middle-High temperature component											
B2 65°50′ N, 88°14′E											
R	42	50.0	3.7	29.6	4.1	46.3	18.7	28.7	4.2		Plat = −25.6 Plong = 36.0 dp/dm = 2.3/4.4
FORMATION TURUKHANSK											
High temperature component											
T1 65°49′N, 88°08′E											
R	17	63.8	−56.9	48.6	5.2	72.2	−28.3	44.6	5.4		
N	18	253.9	58.1	70.0	4.2	257.7	26.3	39.5	5.6		
N + R	35	248.9	57.6	55.0	3.3	255.0	27.3	41.2	3.8		Plat = 7.2 Plong = 17.6 dp/dm = 2.3/4.1
Middle-High temperature component											
T1											
R	20	43.0	−11.9	25.5	6.6	43.0	13.4	26.8	6.4		Plat = −23.9 Plong = 40.3 dp/dm = 3.3/6.5

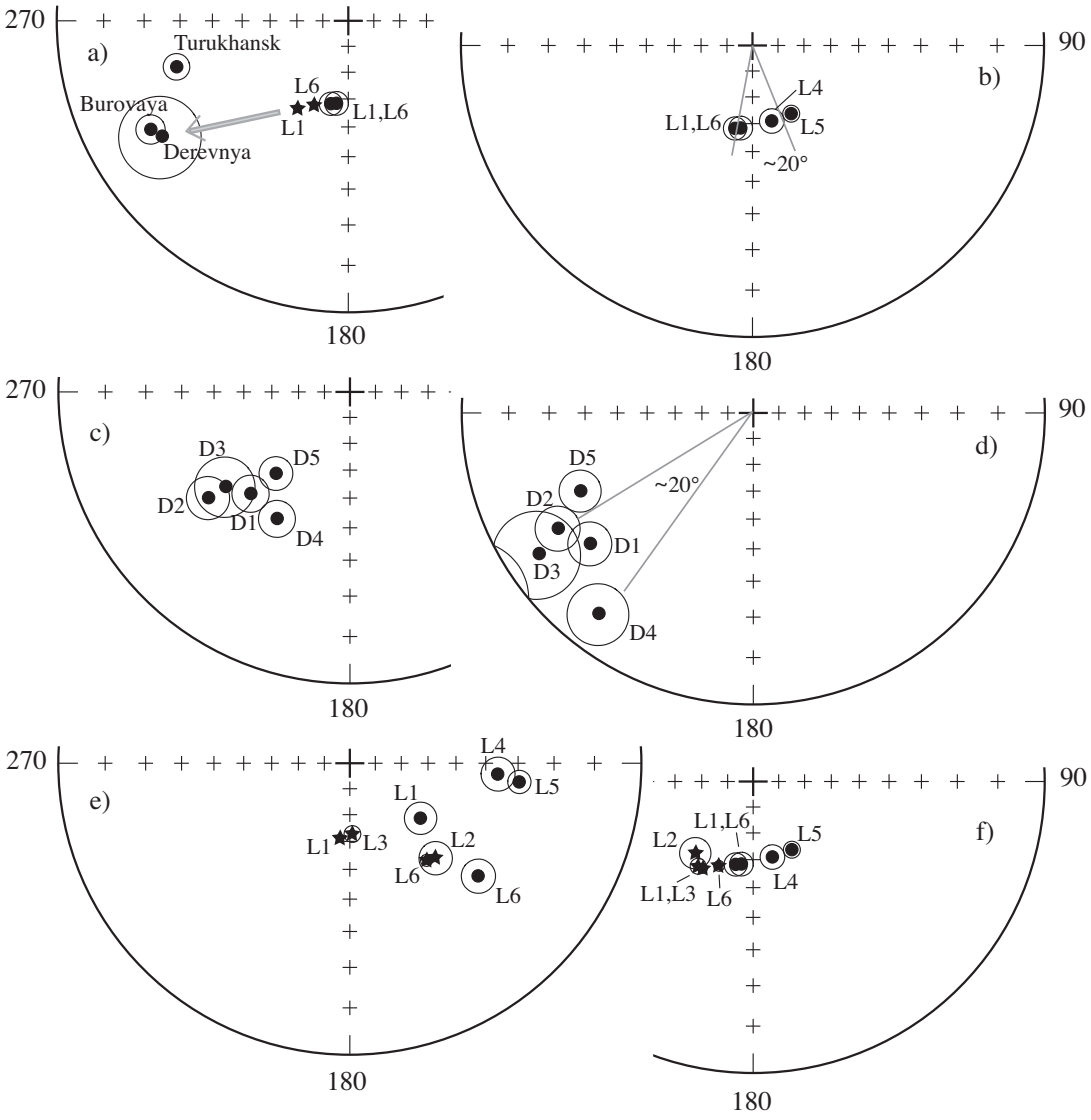

Fig. 12. Stereographic projection of the mean directions of the high unblocking temperature magnetization component obtained in the Linok, Derevnya, Burovaya and Turukhansk formations (see Table 1). (a) Directions obtained from the lower and middle (black circles) and upper (black stars) Linok sub-formations of sections L1 and L6 after bedding correction. The grey arrow indicates that these directions evolve toward the mean directions obtained from the Derevnya and Burovaya formations. (b) Comparison between the directions obtained from the lower and middle Linok sub-formations of sections L1, L4, L5 and L6 after bedding correction. A difference of ~20° in declination is apparent between the directions of L1 and L6 and the directions of L4 and L5. (c) and (d) Directions obtained for the Derevnya Formation before and after bedding correction. A rough difference of ~20° in declination is also apparent after bedding correction between the directions of D1, D2, D3, D5 and the direction of D4 (see text). (e) and (f) Directions obtained for the Linok Formation before and after bedding correction, with a distinction between the directions of the lower and middle sub-formations (black circles) and those from the upper sub-formation (black stars).

carried out on a large collection of samples clearly dismiss a primary (syn-depositional) origin for the magnetization components only isolated at temperatures lower than ~500 °C. In particular, they demonstrate the absence of an exploitable geomagnetic record for the Sukhaya Tunguska Formation. The consequence is that these new data invalidate the reliability of the paleomagnetic poles, defined from only a small number of data, previously proposed (with caution) by Pavlov et al. (2015) for the Sukhaya Tunguska and Miroedikha formations. Pavlov et al. (2015) further suggested the occurrence of magnetic polarity reversals during the deposition of these two formations. It thus appears that this interpretation can no longer be accepted.

It thus arises that geomagnetic polarity reversals are principally observed within the Ln1 and Ln2 Linok sub-formations (Fig. 14 and Fig. S3 in Supplementary material; note that the results from sections L2 and L3 were combined in Fig. 14 as they stratigraphically follow each other). The most complete record was obtained in section L1, with more than a dozen geomagnetic field reversals (see also the data from sections L4 and L5). The latter are mainly concentrated in the upper part of the Ln1 sub-formation and in the lower part of the Ln2 sub-formation (Fig. 14; Fig. S3). The lower part of Ln1 sub-formation predominantly exhibits a reverse polarity. A normal polarity interval begins around the middle of the Ln2 sub-formation, which is then observed throughout

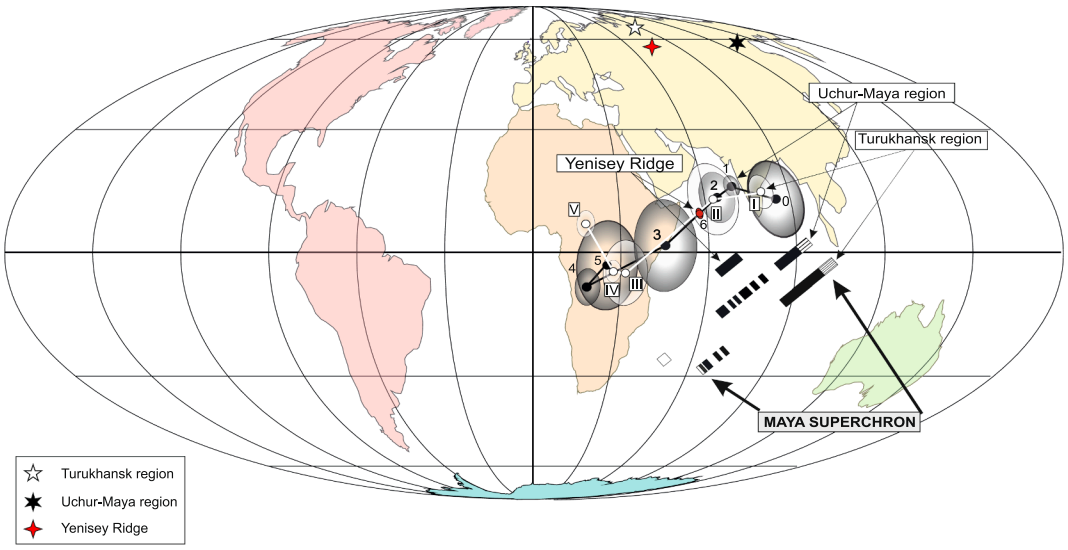

Fig. 13. Comparison between the paleomagnetic poles obtained around the Mesoproterozoic/Neoproterozoic boundary from the Uchur Maya, Yenisey Ridge and the Turukhansk regions (Pavlov, 1994; Pavlov et al., 2000, 2002; Pavlov and Gallet, 2010; Gallet et al., 2012; this study). The new poles from the Turukhansk region are reported in white: I, lower and middle parts of the Linok Formation; II, upper part of the Linok Formation.; III, Derevnya Formation; IV, Burovaya Formation; V, Turukhansk Formation. The black dots indicate the poles from the Uchur Maya region after correction for the closure of the Viluy rift system via a 25° counter-clockwise rotation with a Euler pole at 62°N, 117°E (Pavlov et al., 2008). 0, Totta Formation; 1, Malgina Formation; 2, Tsipanda Formation; 3, Lakhanda Formation; 4, Kandyk sills; 5, Ust-Kirba Formation. The red dot shows the pole obtained for the Kartochka Formation from the Yenisey Ridge region after a 20°-clockwise rotation (Gallet et al., 2012). The composite magnetic polarity sequences established from the different datasets and the probable range of the Maya superchron are also reported on the figure. (For interpretation of the references to color in this figure legend, the reader is referred to the web version of this article.)

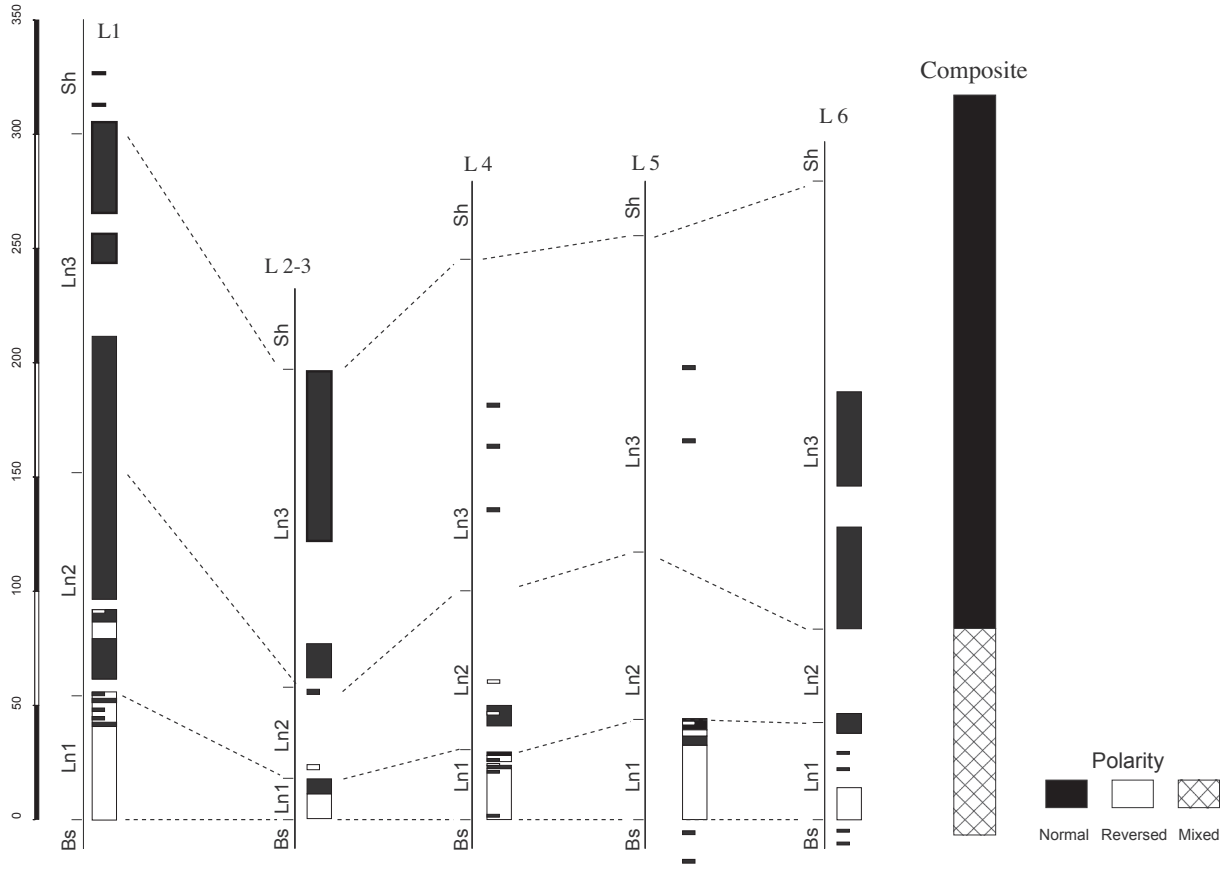

Fig. 14. Magnetic polarity zonation obtained from the different sections of the Linok Formation and construction of a simplified composite polarity sequence.

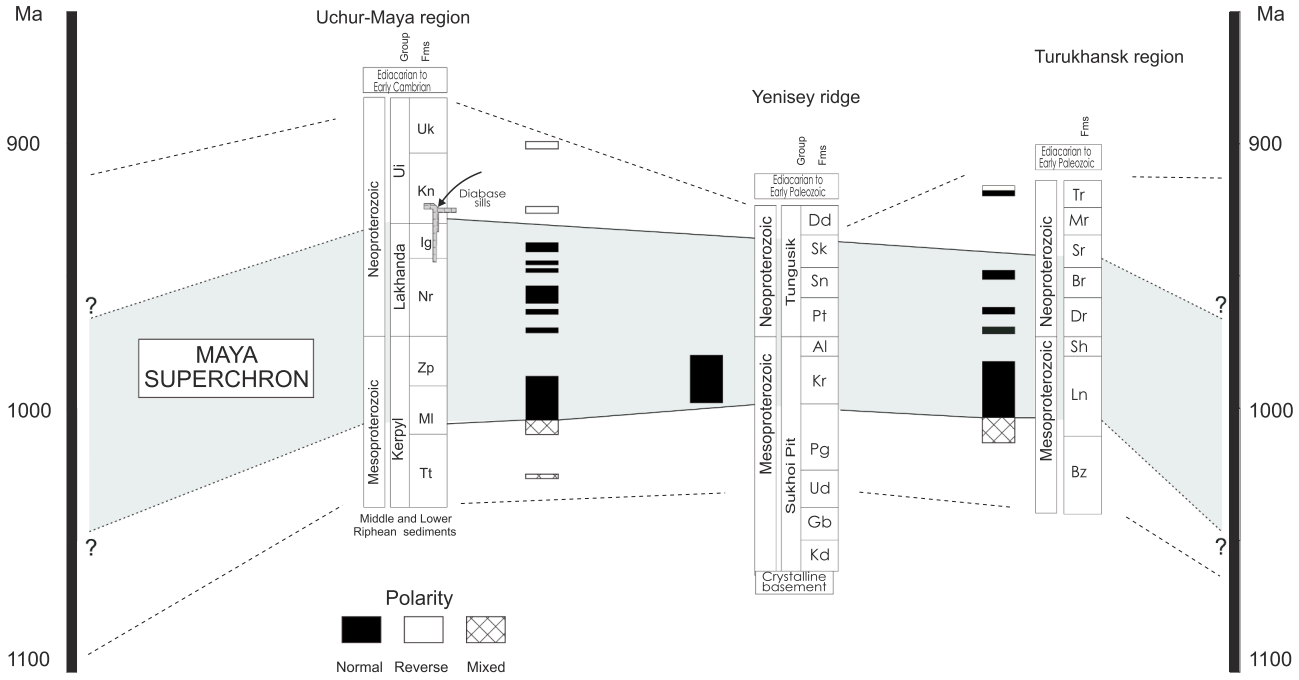

Fig. 15. Comparison between the composite magnetic polarity sequences obtained from the Uchur Maya (Pavlov and Gallet, 2010), the Yenisey Ridge (Gallet et al., 2012) and the Turukhansk (this study) regions. The polarity option is discussed in the text. The dotted lines indicate the approximative time span encompassed by the sequences. This comparison leads to the identification of a superchron of normal polarity (called Maya superchron) encompassing the Mesoproterozoic/Neoproterozoic boundary at ~1 Ga (grey area).

the Ln3 sub-formation. A very fragmentary record of this normal polarity interval (if continuous) is observed up to Turukhansk Formation, where a polarity reversal is observed.

A comparison between the magnetostratigraphic data obtained so far from different Siberian regions (Uchur-Maya, Yenisey Ridge and Turukhansk Uplift regions) is displayed in Fig. 15. The figure is based on the temporal correlation between the Middle-Late Riphean (late Mesoproterozoic-Neoproterozoic) sequences from these regions via lithologic, biostratigraphic, geochemical and radiometric considerations (e.g. Semikhatov and Serebryakov, 1983; see also in Gallet et al., 2012 and references therein). These sequences are expected to have nearly the same age, around 1050–950 Ma. In Fig. 15, we consider simplified composite magnetostratigraphic sequences consisting of normal, reversed and mixed polarity intervals. A good agreement is observed between these different sequences. In all three cases a distinctively long normal polarity interval is detected. This adds another element in favor of the contemporaneity of the different formations. We note that the lower part of the Malgina Formation (referred to as Ml in Fig. 15) has numerous geomagnetic field reversals, however the results do not show a relatively thick reverse interval as is observed in the lower part of the Ln1 sub-formation (Fig. 14; Fig. S3 in Supplementary material). We tentatively suggest that the latter Ln1 interval extends further back in time (see also Pisarevsky and Natapov, 2003).

Next we analyze the paleomagnetic poles obtained from the Uchur-Maya, Yenisey Ridge and Turukhansk regions (Fig. 13). In order to compare the paleomagnetic poles obtained from the Turukhansk and Uchur-Maya regions (in Angara-Anabar reference frame), we consider the opening of the Viluy rift system during the Paleozoic, which consists of rotating by ~25° counterclockwise the poles from the Uchur-Maya region around the Euler pole 62°N, 117°E (e.g. Pavlov et al., 2008; Gallet et al., 2012). In this case, the new poles estimated for the Ln1-Ln2 and Ln3 Linok sub-formations and for the Derevnya, Burovaya and Turukhansk formations show a very similar trend as that defined by the paleomagnetic poles previously obtained from the Totta, Malgina, Lakhanda and Kandyk formations (Fig. 13; Pavlov, 1994; Pavlov et al., 2000; 2002; Pavlov and Gallet, 2010). The pole from the Derevnya and Burovaya formations lie between the poles obtained from the Lakhanda series and from sills intruding (and nearly coeval with) the overlying Kandyk Formation, suggesting similar ages, while the pole from the Turukhansk Formation lies in the continuation after the Kandyk paleomagnetic pole. The case is even more favorable for the pole estimated for the Ln3 Linok sub-formation, because it is in very good agreement with the poles determined for the Malgina and Tsipanda formations. It is also in agreement with the pole from the Kartochka Formation after its rotation (see below; Fig. 13). Finally, the pole obtained for the Ln1–Ln2 Linok sub-formations is slightly different from the Malgina pole. It is in better agreement with the pole previously obtained by Pavlov (1994) for the Totta Formation, which underlies the Malgina Formation (Fig. 15). At this stage, the lower part of the Linok Formation is likely slightly older that the Malgina Formation (as also suggested by Pisarevsky and Natapov, 2003).

Gallet et al. (2012) introduced the comparison between the paleomagnetic poles from the Kartochka and Malgina formations, with the latter being corrected for the Viluy rift opening (Pavlov et al., 2008). A good agreement between them requires an approximate 20° clockwise rotation around a vertical axis of the Kartochka section, belonging to the disturbed margin of the Angara-Anabar block of the Siberian platform (East-Angara terrain). Such a rotation seems plausible at the time of the collision of the Central-Angara terrain with the Angara-Anabar block, likely during the Neoproterozoic period (Vernikovsky and Vernikovskaya, 2006). The overall paleomagnetic results shown in Fig. 13 therefore strongly advocate for a tight temporal correlation between the late Mesoproterozoic formations of the Turukhansk, Uchur-Maya and Yenisey Ridge regions. It is worth remarking that the agreement between poles obtained from very distant regions of the Siberian platform strengthens the strong dipolarity of the geomagnetic field around the Mesoproterozoic and Neoproterozoic boundary.

The normal magnetic polarity interval found in section L1 ranging from the middle of the Ln2 to the end of the Ln3 sub-formations has a stratigraphic thickness of ~200 m (Fig. 14). This may indicate a duration longer than a dozen Myr, considering a sedimentation rate of approximately 1 to 2 cm per 1000 years typical in carbonate platform

environments (e.g. Bosscher and Schlager, 1993). Such a value is also typical of sedimentation rates characterizing Early Paleozoic sections in different Siberian epicontinental basins, which appear comparable to the Turukhansk region (e.g., Gallet and Pavlov, 1996; Pavlov and Gallet, 1998). Given all available magnetostratigraphic data, it is highly probable that this interval, a superchron, lasted for a much longer period (Fig. 15). Unfortunately, the data set from the Siberian platform is still too sparse to precisely constrain this issue. For example, in the Turukhansk region, we could not obtain reliable paleomagnetic results from the dolomitic Sukhaya Tungunska Formation immediately overlying the Linok Formation. Only the sections sampled in the lower and middle parts of the Derevnya Formation deposited after the Sukhaya Tungunska Formation and in one ~75-m thick section (B1) of the Burovaya Formation reveal a normal polarity. This result may indicate a very long extension of the normal polarity interval found in the Linok Formation. This is consistent with the paleomagnetic results, which all show a normal polarity, obtained in several series succeeding the Malgina Formation in the Uchur-Maya region (Fig. 15). Based on the available Siberian data, this interval would then extend on either side of the boundary between the Mesoproterozoic and the Neoproterozoic, which is dated at ca 1 Ga, with a probable duration of several tens of Myr (~50 Myr?; Fig. 15). This rough estimate relies on radiometric data available from the Malgina Formation (1043 ± 14 Ma; Ovchinnikova et al., 2001) and from the Kandyk sills showing a reversed polarity magnetization. These sills were dated at 942 ± 19 Ma by Pavlov et al. (2002) using the Sm-Nd isochron method, whereas other sills not paleomagnetically studied until now were dated between ~930 Ma and ~1000 Ma by Rainbird et al. (1998) (see also Khudoley et al., 2007).

Comparing the results above with the paleomagnetic data dated at ~1 Ga available from other regions does not provide additional information on the duration of the Maya superchron. The amount of data is low and predominantly obtained from the North American (Laurentia) and the Baltic shields. In North America, the most comprehensive paleomagnetic dataset has been obtained from the Keweenawan lava flows dated at ~1.10 Ma (e.g. Halls and Pesonen, 1982; Tauxe and Kodama, 2009; Swanson-Hysell et al., 2009 and references therein). In particular, the results from the Mamainse Point area show a succession of several geomagnetic polarity reversals (Swanson-Hysell et al., 2009). On the other hand, a set of data obtained on the Baltic shield allows one to constrain the period that would correspond with the end of the Maya superchron. There, the paleomagnetic data were mainly obtained from dykes dated around 950–935 Ma (e.g. Pisarevsky and Bylund, 2006; Elming et al., 2014 and references therein). The latter show both magnetic polarities although no succession of magnetic polarity intervals record was established (e.g. Pisarevsky and Bylund, 2006). It is worth mentioning that the occurrence of reversals at that time appears in agreement with the reversed polarity evidenced by Pavlov et al. (2002) from Kandyk sills dated at ~942 Ma (see above). All these data clearly attest that the Maya superchron did not extend after ~950 Ma. There is at present no precisely dated results allowing to further constrain a possible continuous duration of the Maya superchron between ~1050 Ma and ~950 Ma. Driscoll and Evans (2016), in a recent study carried out on a selection of paleomagnetic data contemporaneous in age with the Maya superchron, showed that only Laurentian data from the Jacobsville and Chequamegon Sandstone formations (Roy and Robertson, 1978; McCabe and Van der Voo, 1983), showing respectively a few magnetic polarity reversals and a single reversed polarity, could challenge the long extension of the Maya superchron. This said, Driscoll and Evans (2016) also underlined the poor age control of these formations and, moreover, Malone et al. (2016; 2018) proposed, based on detrital-zircon ages, a much younger age of deposition for these two formations, younger than the end of the Maya superchron.

To summarize, the new magnetostratigraphic data presented in this study are compatible with all previous results obtained from the Uchur Maya (Pavlov and Gallet, 2010) and Yenisey Ridge (Gallet et al., 2012) regions. We assume that the long normal polarity interval identified in the Linok Formation correlates with the Maya superchron, so named because it was first discovered along the Maya river (Pavlov and Gallet, 2010). It is worth mentioning that the occurrence of this superchron is now particularly well constrained by very consistent datasets obtained in distant regions of the Siberian platform, which attests of the principally dipolar nature of the geomagnetic field ~ one billion years ago. The duration of this superchron still remains a matter of debate because only fragmentary geomagnetic field records were obtained up to now both from the Derevnya and Burovaya formations, and from the Lakhanda Group of the Uchur-Maya region (Fig. 15). Deciphering that issue would be particularly important to test whether the Maya superchron lasted a minimum of ~50 Myr, i.e. a duration similar to that of the Kiaman superchron. The other possibility would be that, around one billion years ago, several rather short (< 20 Myr?) superchrons, with a predominantly normal polarity, occurred in a relatively short time interval. We note that such a behavior would constitute an unusual situation relative to the recurrence and duration of superchrons known during the Phanerozoic (e.g. Pavlov and Gallet, 2005). These two options clearly enter the debate about the frequency of superchrons during the Precambrian (Gallet et al., 2012; Driscoll and Evans, 2016). At this stage, however, the absence of polarity reversal at the very beginning of the Neoproterozoic in both the Turukhansk Uplift and Uchur-May regions, an important finding of the present study, tends to favor the first option. In this respect, the acquisition of magnetostratigraphic data for the Neoproterozoic would be a major achievement to further constrain the long-term evolution of the Earth's magnetic field.

7. Conclusions

- Thermal demagnetization of samples collected from the Siberian Late Mesoproterozoic Linok Formation isolates a HT magnetization component carried by magnetite. The syn-sedimentary nature of this magnetization is proven using positive reversal, conglomerate and fold tests. The mean paleomagnetic directions obtained from different sections further indicate Turukhansk block motion during deposition of the Linok Formation, as well as a counterclockwise rotation of ~20° of the northern part of this block relative to its southern part.
- Thermal demagnetization carried out on samples from the Early Neoproterozoic Burovaya and Turukhansk formations reveals a HT (> ~500 °C) magnetization component carried by magnetite and hematite, respectively. No magnetic polarity reversal is observed from the Burovaya samples, whereas those from the Turukhansk Formation show a single polarity reversal.
- New analysis of demagnetization data from the Derevnya Formation underlying the Burovaya Formation does also not show the presence of magnetic polarity reversals. Evidences for the primary (early diagenetic) origin of the mean HT directions obtained for the Derevnya and Burovaya formations include the facts that they lie in the continuity of the directional evolution observed through the Linok Formation, and that the corresponding paleomagnetic poles are in good agreement with other poles assumed to be similar in age previously obtained from the Uchur-Maya region.
- A magnetization component isolated in the moderate temperature range (up to ~350–400 °C) is consistently observed in all formations of the Turukhansk Uplift region. We propose that this component was acquired in a reversed polarity field during the Kiaman Permo-Carboniferous superchron.
- A magnetization component is isolated between ~400 °C and ~500 °C in samples from the Burovaya and Turukhansk formations. This component was likely acquired before folding, therefore before the end of the Neoproterozoic.
- The remagnetization components isolated < ~500 °C, together with new demagnetization data obtained from the Sukhaya Tunguska

Formation invalidate the preliminary interpretation tentatively made by Pavlov et al. (2015) from a small collection of samples on the occurrence of magnetic polarity reversals during deposition of the Sukhaya Tunguska and Miroedikha formations.

- Geomagnetic polarity reversals are observed in the lower part of the Linok Formation, whereas a single polarity interval occurs through its upper part, over a stratigraphic thickness of ~200 m. The paleomagnetic data obtained in the Derevnya and Burovaya formations have the same polarity. According to previous studies, this magnetic interval would possess a normal polarity.
- The long normal polarity interval found in the Linok Formation is likely a superchron, which lasted more than a dozen of Myr.
- The new magnetostratigraphic results are consistent with previous data obtained from the Siberian Malgina (Pavlov and Gallet, 2010) and Kartochka (Gallet et al., 2012) formations. The contemporaneity of the different sections is further attested by the excellent agreement observed between their paleomagnetic poles, with a similar APWP track.
- The analysis suggests that the superchron found in the Linok Formation is the Maya superchron dated to ca 1 Ga.

Acknowledgments

This study was financed by grants #14.Z50.31.0017 and #14.Y26.31.0029 of the Ministry of Science and High Education of the Russian Federation and by the INSU-CNRS program PNP. The maintenance of the laboratory equipment at IPE-RAS was made possible by grant #161710097 of the Russian Science Foundation. The paper was partly written while VP benefited from the invitation program of IPGP and with the support of grant #18-05-00285 of the Russian Foundation for Basic Research. We thank Galen Halverson for his help on the field. We are grateful to S. Pisarevsky and an anonymous reviewer for helpful comments on our manuscript. This is IPGP contribution no. 3990.

Appendix A. Supplementary data

Supplementary data to this article can be found online at https://doi.org/10.1016/j.precamres.2018.11.005.

References

Aubert, J., Labrosse, S., Poitou, C., 2009. Modelling the palaeo-evolution of the geodynamo. Geophys. J. Int. 179, 1414–1428.
Bachtadse, V., Pavlov, V.E., Kazansky, A.Y., Tait, J.A., 2000. Siluro-Devonian paleomagnetic results from the Tuva Terrane (southern Siberia, Russia): implications for the paleogeography of Siberia. J. Geophys. Res. 105 (B6), 13509–13518.
Bartley, J.K., Semikhatov, M.A., Kaufman, A.J., Knoll, A.H., Pope, M.C., Jacobsen, S.B., 2001. Global events across the Mesoproterozoic-Neoproterozoic boundary: C and Sr isotopic evidence from Siberia. Precambr. Res. 111, 165–202.
Biggin, A.J., Piispa, E.J., Pesonen, L.J., Holme, R., Paterson, G.A., Veikkolainen, T., Tauxe, L., 2015. Palaeomagnetic field intensity variations suggest Mesoproterozoic inner-core nucleation. Nature 526, 245–248.
Bosscher, H., Schlager, W., 1993. Accumulation rates of Carbonate platforms. J. Geol. 417 (101), 345–355.
Cogné, J.-P., 2003. PaleoMac: a MacIntosh@ application for treating paleomagnetic data and making plate reconstructions. Geochem. Geophys. Geosyst. 4, 1007.
Cocks, L.R.M., Torsvik, T.H., 2007. Siberia, the wandering northern terrane, and its changing geography through the Palaeozoic. Earth-Sci. Rev. 82, 29–74.
Driscoll, P., Evans, D., 2016. Frequency of Proterozoic geomagnetic superchrons. Earth Planet. Sci. Lett. 437 (1), 9–14.
Dunlop, D.J., Yu, Y.J., 2004. Intensity and polarity of the geomagnetic field during Precambrian time. In: Channell, J.E.T., Kent, D.V., Lowrie, W., Meert, J.G. (Eds.), Timescales of the Paleomagnetic Field. American Geophysical Union, Geophysical Monograph Series, pp. 85–100.
Elming, S.A., Pisarevsky, S.A., Layer, P., Bylund, G., 2014. A paleomagnetic and 40Ar/39Ar study of mafic dykes in southern Sweden: a new Early Neoproterozoic key-pole for the Baltic Shield and implications for Sveconorwegian and Grenville loops. Precambr. Res.
Elston, D.P., Enkin, R.J., Baker, J., Kisilevsky, D.K., 2002. Tightening the Belt: paleomagnetic-stratigraphic constraints on deposition, correlation, and deformation of the Middle Proterozoic (ca. 1.4 Ga) Belt-Purcell Supergroup. United States and Canada. GSA Bullet. 114, 619–638.
Enkin, R., 2003. The direction-correction tilt test: an allpurpose tilt/fold test for paleomagnetic studies. Earth Planet Sci. Lett. 212, 151–166.
Gallet, Y., Pavlov, V., 1996. Magnetostratigraphy of the Moyero river section (northwestern Siberia): constraints on geomagnetic reversal frequency during the early Paleozoic. Geophys. J. Int. 125, 95–105.
Gallet, Y., Pavlov, V., Semikhatov, M., Petrov, P., 2000. Late Mesoproterozoic magnetostratigraphic results from Siberia: paleogeographic implications and magnetic field behavior. J. Geophys. Res. 105 (16), 481–16499.
Gallet, Y., Pavlov, V., Halverson, G.P., Hulot, G., 2012. Toward constraining the long-term reversing behavior of the geodynamo: a new "Maya" superchron ~1000 Ma ago from the magnetostratigraphy of the Kartochka Formation (southwestern Siberia). Earth Planet. Sci. Lett. 339–340, 117–126.
Gallet, Y., Pavlov, V.E., 2016. Three distinct reversing modes in the Geodynamo Izvestiya. Phys. Solid Earth 52 (2), 291–296.
Gorokhov, I.M., Semikhatov, M.A., Baskakov, A.V., Kutyavin, E.P., Mel'nikov, N.N., Sochava, A.V., Turchenko, T.L., 1995. Sr isotopic composition in Riphean, Vendian, and Lower Cambrian carbonates from Siberia. Stratigr. Geol. Correl. 3, 1–28.
Halls, H., Pesonen, L., 1982. Paleomagnetism of Keweenawan rocks. Geol. Soc. Am. Mem. 156, 173–201.
Irving, E., Baker, J., Hamilton, M., Wynne, P., 2004. Early Proterozoic geomagnetic field in western Laurentia: implications for paleolatitudes, local rotations and stratigraphy. Precambr. Res. 129 (3), 251–270.
Jacobs, J.A., 2001. The cause of superchrons. Astron. Geophys. 42 (6), 30–31.
Kaurova, O.K., Ovchinnikova, G.V., Gorokhov, I.M., 2010. U-Th-Pb systematics of Precambrian carbonate rocks: dating of the formation and transformation of carbonate sediments. Stratigr. Geol. Correl. 18 (3), 252–268.
Khudoley, A., Kropachev, A., Tkachenko, V., Rublev, A., Sergeev, S., Matukov, D., Lyahnitskaya, O., 2007. Mesoproterozoic to Neoproterozoic evolution of the Siberian craton and adjacent microcontinents: an overview with constraints for a Laurentian connection. Spec. Publ. SEPM Soc. Sediment. Geol. 86, 209–226.
Kirschvink, J.L., 1980. The least-squares line and plane and the analysis of paleomagnetic data. Geophys. J. R. Astr. Soc. 62, 699–718.
Knoll, A.H., Kaufman, A.J., Semikhatov, M.A., 1995. The carbon-isotopic composition of Proterozoic carbonates: Riphean succession from Northwestern Siberia (Anabar massif, Turukhansk uplift). Am. J. Sci. 295, 823–850.
Konôpková, Z., McWilliams, R.S., Gómez-Pérez, N., Goncharov, A.F., 2016. Direct measurement of thermal conductivity in solid iron at planetary core conditions. Nature 534, 99–101.
Kravtsov, A.G., 1967. Tectonics of the Khantayka–Sigovaya region (in Russian). Geol. North-Western Siberian Platform. Trans. Arctic Geol. Inst. 133, 94–106.
Kuznetsov, A.B., Bekker, A., Ovchinnikova, G.V., Gorokhov, I.M., Vasilyeva, I.M., 2017. Unradiogenic strontium and moderate-amplitude carbon isotope variations in early Tonian seawater after the assembly of Rodinia and before the Bitter Springs Excursion. Precambr. Res. 298, 157–173.
Labrosse, S., 2003. Thermal and magnetic evolution of the Earth's core. Phys. Earth Planet. Inter. 140, 127–143.
Landeau, M., Aubert, J., Olson, P.L., 2017. The signature of inner-core nucleation on the geodynamo. Earth Planet. Sci. Lett. 465, 193–204.
Lowrie, W., 1990. Identification of ferromagnetic minerals in a rock by coercivity and unblocking temperature properties. Geophys. Res. Lett. 17, 159–162.
Malone, D.H., Stein, C.A., Craddock, J.P., Kley, J., Stein, S., Malone, J.E., 2016. Maximum depositional age of the Neoproterozoic Jacobsville Sandstone, Michigan: implications for the evolution of the Midcontinent Rift. Geosphere 12 (4), 1–12.
Malone, D.H., Stein, C.A., Craddock, J.P., Kley, J., Stein, S., Malone, J.E., 2018. Maximum depositional age of the Neoproterozoic Jacobsvil Sandstone, Michigan: implications for the evolution of the Midcontinent Rift (Reply). Geosphere 14 (3), 1382–1384.
McCabe, C., Van der Voo, R., 1983. Paleomagnetic results from the upper Keweenawan Chequamegon Sandstone: implication for red bed diagenesis and late Precambrian apparent polar wander of North America. Can. J. Earth Sci. 20, 105–112.
McElhinny, M.W., 1964. Statistical significance of the fold test in palaeomagnetism. Geophys. J. R. Astron. Soc. 8, 338–340.
McFadden, P., McElhinny, M., 1990. Classification of the reversal test in palaeomagnetism. Geophys. J. Int. 103, 725–729.
Mikutskiy, S., Petrakov, V., 1961. Tectonics of Peri-Eniseyan part of North of the Siberian Platform. Trans. Siberian Inst. Geol. Min. Resour. 7, 46–57 (in Russian).
Nikishin, A.M., Sobornov, K.O., Prokopiev, A.V., Frolov, S.V., 2010. Tectonic evolution of the Siberian Platform during the Vendian and Phanerozoic. Moscow Univ. Geol. Bull. 65 (1), 1–16.
Olson, P., Deguen, R., Hinnov, L.A., Zhong, S., 2013. Controls on geomagnetic reversals and core evolution by mantle convection in the Phanerozoic. Phys. Earth Planet. Inter. 214, 87–103.
Ovchinnikova, G.V., Semikhatov, M.A., Gorokhov, I.M., et al., 1995. U-Pb Systematics of Precambrian Carbonates: Riphean Sukhaya Tunguska Formation of the Turukhansk Uplift, Siberia. Lithol. Mineral Resourc. 5, 525–536.
Ovchinnikova, G., Semikhatov, M.A., Vasil'eva, I., Gorokhov, I.M., Kaurova, O., Podkovyrov, V., Gorokhovskii, B., 2001. Pb–Pb age of carbonates from the middle Riphean Malga Formation, Uchur-Maya region of east Siberia. Stratigr. Geol. Correl. 9, 3–16.
Pavlov, V.E., 1994. The paleomagnetic poles from the riphean uchuro-maiskii hypostratotype and the riphean drift of the aldan block. Siberian Platform. Dokl. Ross. Akad. Nauk. 336 (4), 533–537.
Pavlov, V.E., Petrov, P.Yu., 1996. Paleomagnetic study of Riphean deposits in the Turukhansk area Izvestiya. Phys. Solid Earth 32 (3), 239–249.
Pavlov, V., Gallet, Y., 1998. Upper Cambrian to Middle Ordovician magnetostratigraphy from the Kulumbe river section (northwestern Siberia). Phys. Earth Planet. Inter. 108, 49–59.
Pavlov, V.E., Gallet, Y., Shatsillo, A.V., 2000. Paleomagnetism of the Upper Riphean

Lakhandinskaya Group in the Uchuro-Maiskii area and the hypothesis of the Late Proterozoic supercontinent. Izvestiya Phys. Solid Earth 36 (8), 638–648.
Pavlov, V.E., Gallet, Y., Petrov, P.Yu., Zhuravlev, D.Z., Shatsillo, A.V., 2002. The Ui group and Late Riphean sills in the Uchur–Maya area: isotope and paleomagnetic data and the problem of the rodinia supercontinent. Geotectonics 36 (4), 278–292.
Pavlov, V., Gallet, Y., 2005. A third superchron during the Early Paleozoic. Episodes 28 (2), 78–84.
Pavlov, V., Bachtadse, V., Mikhailov, V., 2008. New Middle Cambrian and Middle Ordovician palaeomagnetic data from Siberia: Llandeilian magnetostratigraphy and relative rotation between the Aldan and Anabar-Angara blocks. Earth Planet. Sci. Lett. 276 (3–4), 229–242.
Pavlov, V., Gallet, Y., 2010. Variations in geomagnetic reversal frequency during the Earth's middle age. Geochem. Geophys. Geosyst. 11, Q01Z10.
Pavlov, V.E., Shatsillo, A.V., Petrov, P.Yu., 2015. Paleomagnetism of the upper Riphean deposits in the Turukhansk and Olenek uplifts and Uda Pre-Sayan region and the neoproterozoic drift of the Siberian Platform. Izvestiya Phys. Solid Earth 51 (5), 716–747.
Petrov, P.Yu., Veis, A.F., 1995. Facial-ecological structure of the Derevnya Formation microbiota: upper Riphean, Turukhansk Uplift. Siberia. Stratigr. Geol. Correl. 3, 435–460.
Petrov, P.Yu., 1993. Structure and sedimentation conditions of the lower Riphean formations in the northern part of the Turukhansk Uplift. Siberia. Stratigr. Geol. Correl. 1 (2), 55–66.
Petrov, P.Yu., 2000. The clayey-carbonate sedimentation cycle and carbonate platform formation: evidence from the Linok formation, the middle Riphean of the Turukhansk Uplift Siberia. Lithol. Mineral Resourc. 35 (3), 232–251.
Petrov, P.Yu., Semikhatov, M.A., 2001. Sequence organization and growth patterns of late Mesoproterozoic stromatolite reefs: an example from the Burovaya Formation, Turukhansk Uplift Siberia. Precambr. Res. 111 (1–4), 257–281.
Petrov, P.Yu., Semikhatov, M.A., 2005. Specific Development of the Late Riphean Siliciclastic-Carbonate Shelf: the Derevnya Formation of the Turukhansk Uplift, Siberia, and Lithostratigraphic Equivalents. Stratigr. Geol. Correl. 13, 242–263.
Petrov, P.Yu., Semikhatov, M.A., 2009. Platforms: Shorikha Formation of the Turukhansk Uplift Siberia. Stratigr. Geol. Correl. 17 (5), 461–475.
Petrov, P.Yu., 2016. Molar Tooth Structures and Origin of Peloids in Proterozoic Carbonate Platforms (Middle Riphean of the Turukhansk Uplift, Siberia). Lithol. Mineral Resourc. 51 (4), 290–309.
Pisarevsky, S.A., Bylund, G., 2006. Palaeomagnetism of 935 Ma mafic dykes in southern Sweden and implications for the Sveconorwegian Loop. Geophys. J. Int. 166, 1095–1104.
Pisarevsky, S.A., Natapov, L.M., 2003. Siberia and Rodinia. Tectonophysics 375, 221–245.
Pozzo, M., Davies, C., Gubbins, D., Alfè, D., 2012. Thermal and electrical conductivity of iron at Earth's core conditions. Nature 485, 355–358.
Rainbird, R., Stern, R., Khudoley, A., Kropachev, A., Heaman, L., Sukhorukov, V., 1998. U-Pb geochronology of Riphean supracrustal rocks from southeast Siberia and its bearing on the Laurentia-Siberia connection. Earth Planet. Sci. Lett. 164, 409–420.
Roberts, N., Piper, J., 1989. A Description of the Behaviour of the Earth's Magnetic Field. In: Jacobs, J. (Ed.), Geomagnetism. 3. Elsevier, New York, pp. 163–260.
Roy, J.L., Robertson, W.A., 1978. Paleomagnetism of the Jacobsville Formation and the Apparent Polar Path for the interval -1100 to -670 m.y. for North America. J. Geophys. Res. 83 (B3), 1289–1304.
Semikhatov, M.A., Serebryakov, S.N., 1983. The Siberian Hypostratotype of the Riphean. Nauka, Moscow, 367, 224 pp. (In Russian).
Semikhatov, M.A., Ovchinnikova, G.V., Gorokhov, I.M., Kuznetsov, A.B., Vasil'eva, I.M., Gorokhovskii, B.M., Podkovyrov, V.N., 2000. Isotopic age of the Middle–Upper Riphean boundary: Pb–Pb geochronology of the Lakhanda Group carbonates, Eastern Siberia. Dokl. Earth Sci. 372 (2), 625–629.
Sergeev, V.N., 2006. Precambrian microfossils in cherts: their paleobiology, classification, and biostratigraphic usefulness. Geos, Moscow, pp. 280 (in Russian).
Shatsillo, A.V., Fedukin, I.V., Pavlov, V.E. 2012. Paleomagnetism of the Late Devonian and Early Carboniferous of the Minusa depressions and the problem of elaboration of the Middle-Paleozoic segment of the Siberian platform. In: Shcherbakov, V.P. (Ed.) Paleomagnetism and rock-magnetism (theory, practice, experiment). Transactions of the international school-seminar "Problems of paleomagnetism and rockmagnetism". Publishing house "Solo". S.Petersbourg. 270-277. (In Russian).
Shipunov, S.V., 1997. Synfolding magnetization: detection, testing and geological applications. Geophys. J. Int. 130 (2), 405–410.
Smirnov, A.V., Tarduno, J.F., Kulakov, E.V., McEnroe, S.A., Bono, R.K., 2016. Palaeointensity, core thermal conductivity and the unknown age of the inner core. Geophys. J. Int. 205, 1190–1195.
Swanson-Hysell, N.L., Maloof, A.C., Weiss, B.P., Evans, D.A.D., 2009. No asymmetry in geomagnetic reversals recorded by 1.1-billion-year-old Keweenawan basalts. Nat. Geosci. 2, 713–717.
Tauxe, L., Kodama, K.P., 2009. Paleoseculr variation models for ancient times: clues from Keweenawan lava flows. Phys. Earth Planet. Inter. 177, 31–45.
Torsvik, T.H., van der Voo, R., Preeden, U., Mac Niocaill, C., Steinberger, B., Doubrovine, P.V., van Hinsbergen, D.J.J., Domeier, M., Gaina, C., Tohver, E., Meert, J.G., McCausland, P.J.A., Cocks, L.R.M., 2012. Phanerozoic polar wander, paleogeography and dynamics. Earth Sci. Rev. 114, 325–368.
Vernikovsky, V.A., Vernikovskaya, A.E., 2006. Tectonics and evolution of granitoid magmatism in the Yenisei Ridge. Russ. Geol. Geophys. 47 (1), 32–50.
Watson, G.S., 1956. A test for randomness of directions. Geophys. J. Int. 7 (4), 160–161.
Wicht, J., Hori, K., Dietrich, W., Manglik, A., 2011. Numerical models of the early geodynamo, Abstracts, American Geophysical Union Fall Meeting 2011, UI13A_0023.
Zonenshain, L.P., Kuzmin, M.I., Natapov, L.M., 1990. Geology of the USSR: A Plate-Tectonic Synthesis. In: Benjamin, M. (Ed.), Page Geodynamics Series 21. American Geophysical Union Washington, D.C, pp. 242.